

THESIS ON MECHANICAL AND INSTRUMENTAL ENGINEERING E35

Microstructural Aspects of Thermal Sprayed WC-Co Coatings and Ni-Cr Coated Steels

PRIIDU PEETSALU

TUT
PRESS

TALLINN UNIVERSITY OF TECHNOLOGY
Faculty of Mechanical Engineering
Department of Materials Engineering

Dissertation was accepted for the defence of the degree of Doctor of Philosophy in Engineering on October 23, 2007

Supervisor: Prof. Priit Kulu, Faculty of Mechanical Engineering, Department of Materials Engineering

Internal supervisor: Prof. Michal Besterci, Institute of Materials Research, Slovak Academy of Sciences, Košice, Slovakia

Opponents: Senior Research Scientist PhD. Mart Viljus, Materials Research Centre, Tallinn University of Technology

Prof. Lifeng Zhang Department of Materials Science and Engineering, Norwegian University of Science and Technology, Trondheim, Norway

Prof. Toomas Pihl, Tallinn University of Applied Sciences

Defence of the thesis: December 21, 2007

Declaration:

Hereby I declare that this doctoral thesis, my original investigation and achievement, submitted for the doctoral degree at Tallinn University of Technology has not been submitted for any academic degree.

Copyright: Priidu Peetsalu, 2007

ISSN 1406-4758

ISBN 978-9985-59-746-0

CONTENTS

INTRODUCTION.....	8
LIST OF ORIGINAL PUBLICATIONS	9
1 REVIEW OF THE LITERATURE.....	10
1.1 Microstructural evaluation of powders and coatings	10
1.2 Safety belt tongue production and steel microstructure studies methods .	12
1.2.1 Production technology of safety belt tongues.....	13
1.2.2 Microstructural evaluation of steel C60E.....	16
1.3 Objectives and scientific novelty of the study	17
2 EXPERIMENTAL	18
2.1 Powders and coatings.....	18
2.1.1 Composite powder production and particle size analysis.....	18
2.1.2 Thermal spraying of coating.....	19
2.2 Steel C60E	19
2.3 Methods for structure, chemical composition, and phase analysis.....	20
2.4 Methods for mechanical testing.....	21
2.4.1 Tensile and bend tests.....	21
2.4.2 Wear resistance testing	22
3 RESULTS AND DISCUSSION	23
3.1 Characterization of powders and coatings	23
3.1.1 Granularity and morphology of initial and spray powder	23
3.1.2 Phase analysis of powders and coatings	27
3.1.3 Microstructure and porosity analysis	28
3.2 Structural aspects of the Ni-Cr coated steel in the production of safety belt tongues	33
3.2.1 Describing of steel C60E structure at the annealed condition.....	33
3.2.2 Describing of the non-metallic inclusions in the thin sheet metal according to the DIN 50602	42
CONCLUSIONS.....	45
KOKKUVÕTE.....	46
REFERENCES.....	49
List of publication of author	55
ABSTRACT	58
ELULOOKIRJELDUS	59
CURRICULUM VITAE	61

SYMBOLS, DEFINITIONS AND ABBREVIATIONS

- A - Grain area on the projection
- A80 - Ultimate elongation of non-proportional test pieces, %
- A_{e1} - Eutectoid phase transformation line at equilibrium, °C
- A_{e3} - Fully austenitic transformation line at equilibrium, °C
- Ag - Uniform elongation, %
- AS - Aspect ratio, ellipticity of the particle, ratio between major and minor axes of the Legendre ellipse
- AS_{mod} - Modified aspect ratio
- Avg - Average ferret
- BET - Brunauer-Emmett-Teller method for specific surface area calculations
- D - Spherical diameter 1.22474 times circular diameter
- d₅₀ - Grain size median diameter
- Dc - Average diameter of particle size by count distribution
- dm - Average grain size diameter measured by 5 degree intervals around centroid
- DM - Disintegrator Milling
- DP - Roughness, dispersion is defined as the ratio of the convex perimeter to the perimeter
- Dv - Average diameter of particle size by volume distribution
- EDS - Energy Dispersive Spectroscopy (for X-ray Microanalysis)
- EX - Arithmetic average
- f_{ic} - Count distribution
- f_{iv} - Volume distribution
- F_v - Volume fraction concrete size class
- f_v - Volume density
- G - Grain size index according to chosen standard (DIN 50601, ISO 643, ASTM E-112)
- HVOF - High Velocity Oxygen Fuel Thermal Spray Process
- IP - Irregularity and ellipticity Parameter, ratio between minimum circumscribed and maximum inscribed circles of the particle cross-section
- IPS - Image Pro 1.3 image analysis system
- K - Non-metallic inclusion content according to DIN 50602 using K method to show the total content of inclusion (K1 and K4 starting rating classes accordingly 1 and 4).
- M - Non-metallic inclusion content according to DIN 50602, M-method to show the largest inclusions (M2 and M3 accordingly largest inclusion to rating classes 2 and 3)
- MAS - Mechanically Activated Synthesis
- M_s - Martensite start temperature, °C
- MX - Mode of distribution function
- OMS - Omnimet Image Analysis System Version 4.1
- P - Grain perimeter on the projection
- R_m - Tensile strength, N/mm²

RN - Roundness is defined as $4\pi \cdot \text{area} / (\text{perimeter squared})$
R_{p0.2} - Yield strength, N/mm²
S - Surface area
SEM - Scanning Electron Microscopy
THT - Steel Technical Delivery conditions
WDS - Wavelength Dispersive Spectroscopy (for X-ray Microanalysis)
XRD - X-Ray Diffraction
 ρ - Density of material

INTRODUCTION

In ancient times blacksmiths made tools of good quality, sometimes these turned out even better than today. This is what we have learnt when investigating the structure of knives. Today we have powerful tools and extensive knowledge in the field of metallography but still there is very much undiscovered, moreover, many relationships between the structure and the properties of a material are difficult to explain. In a way, we do the same as blacksmiths in ancient times – we forge an object, test how it works and if it works we will try to bring a sacrifice to the same God.

Connections between material structure and properties are the subject analyzed in this thesis to make the decisions based on calculations. Structure analysis is based on two types of materials (WC-Co and low alloy steel C60E) in terms of technology and properties.

Thermal sprayed coatings have a wide range of applications, for instance, from the repair of damaged details during maintenance to the production of new details with high wear resistance. Studies of WC-Co system material composite powder for HVOF thermal coatings to achieve dry abrasive wear resistance are conducted in the Department of Materials Engineering of Tallinn University of Technology. It is necessary to describe the powders in a new way because the developments in the production of mechanically activated nano-structured composite powders are a promising area for thermal spray powders.

Steel production has to adapt to the changes due to the globalization of the world market of steel. The prices of steel materials are increasing, therefore new material options are sought for to keep the prices at the same level. This leads to certain changes in factories that consume steel. One of the steps taken to reduce the price is to change the chemical composition and production of steel C60E.

Steel C60E is used to produce safety belt tongues in *AS Norma* and in other TIER-2 suppliers (second level suppliers). Main technologies used in the production of safety belt tongues are fineblanking, austempering and electroplating. C60E has to be suitable for these operations and also acceptable for steel production. During fineblanking and heat treatment, the material composition and microstructure of the material are important factors.

Acknowledgements

I would like to express special thanks to my family and friends for their direct and indirect support and understanding of long working hours. I had very fruitful co-operation with *AS Norma* staff and grate support has been students working with me. Finally I would like to thank my supervisor and Tallinn University of Technology staff for shared experience and hot discussions.

LIST OF ORIGINAL PUBLICATIONS

- I. **Peetsalu, P.**, Zimakov, S., Pirso, J., Mikli, V., Tarbe, R., Kulu, P. Technology and Characterization of Composite Thermal Spray Powders. – *J. Materials Science (Medžiagotyra)*. 2005, 11(4), pp. 385–389
- II. **Peetsalu, P.**, Zimakov, S., Pirso, J., Mikli, V., Tarbe, R., Kulu, P. Characterization of WC-Co Thermal Spray Coatings Based on the Composite Powders. – *Powder Metallurgy Progress, Journal of Science and Technology of Particle Materials*. 2006, 6(1), pp. 34–41
- III. Zimakov, S., Goljandin, D., **Peetsalu, P.**, Kulu, P. Metallic Powders Produced by the Disintegrator Technology. – *International Journal of Materials and Product Technology*. 2007, 28(3/4), pp. 226–251
- IV. **Peetsalu, P.**, Saarna, M., Valdek, M., Juurma, M. Computer Based Steel Microstructure Analysis Describing the Size and Distribution of Structure Phases. – *Acta Metallurgica Slovaca*. 2007, 13(1), pp. 91–95

Approbation

1. The 4th International DAAAM Conference "INDUSTRIAL ENGINEERING - INNOVATION AS COMPETITIVE EDGE FOR SME", 29–30 April 2004, Tallinn, ESTONIA
2. Euro PM2005 Powder Metallurgy Congress & Exhibition, 2–5 October 2005, Prague, Czech Republic
3. Euro PM2006 Congress & Exhibition, 23–25 October 2006, Ghent, Belgium
4. The 15th International Baltic Conference "Engineering Materials&Tribology" BALTMATTRIB-2006, 5–6 October 2006 Tallinn, Estonia
5. 13th International Symposium on Metallography, Metallography 2007, 2–4 May 2007 Stará Lesná, Poprad, Slovak Republic
6. The 7th International Conference on Clean Steel 2007, 4–6 June 2007 Balatonfüred, Hungary

Author's own contribution

The work for this thesis has been accomplished as a team work. Author's contribution is composed of the structure analysis and the required metallographic preparations. Material development and the analysis of the results have been conducted in the framework of team work.

In Papers I, II and III, the characterization of coatings and powders was my contribution. Here Valdek Mikli provided a great help, especially with the SEM analysis.

Steel structure analysis (Paper IV) and tests were made in cooperation with *AS Norma* staff. My role in this work was to lead the project and work out the test plans to solve their challenges in terms of materials. The methods described in Paper IV were developed in cooperation with the master students Eha Kulper and Kaarin Ratas under my supervision.

1 REVIEW OF THE LITERATURE

Metallography is the science dealing with the constitution and structure of metals and alloys as revealed to the unaided eye or by using such tools as low-power magnification, optical microscopy, electron microscopy, and diffraction or x-ray techniques [1]. Nowadays more and more computer aided structure analysis methods are used. The analysis programs can give lot of information in short time but the requirements to the structure image are stricter. Humans can imagine the grains or grain borders in the structure, whereas computers cannot. It has to be based on some algorithm [2]. To investigate material properties, one needs a lot of data about material characteristics, like chemical and phase composition, mechanical properties and material production or exploitation. There are several methods to find out certain material characteristics, but it is necessary to choose the right one for the material from handbooks [3–4].

Metallographic preparation is a subject underestimated in the metallography. However, without good metallographic preparation, the results may be incorrect or it might prove impossible to analyze a material, especially with computer programs. Commercial databases of metallographic consumables producers [5–8] have been helpful for metallographic preparation. In the case of etching, a number of George F. Vander Voort's articles have been used and he has even been consulted as *Buehler Ltd* specialist in the field of metallography [9–15]. Etching procedures are a very important step to establish different structure elements, phases or even phases before the phase transmission (austenite grain size with low alloy steel). The size and shape of the structure phase have to reflect the real structure.

1.1 Microstructural evaluation of powders and coatings

To describe particle size and shape, the image analysis method is commonly used. The powder metallurgy research group of TUT conducted the image analysis by an image processing system consisting of SEM and IPS. To characterize particle size and shape, the following parameters have been used and investigated for particle size characterization:

- mean diameter d_m , μm is the average from distances between particle centroid and particle boundary measured by five degree intervals around centroid;
- cumulative volume distribution function of the particles volume;
- median diameter d_{50} , which corresponds to the half of the total content of powder obtained from the cumulative distribution function;
- volume density function f_v calculated by Eq. (1.1):

$$f_v = \frac{F_v^{i+1} - F_v^i}{\log d_{i+1} - \log d_i} \quad (1.1)$$

To characterize particle shape the following considerations are used:

- aspect ratio (ellipticity) AS reports the ratio between the major axis and the minor axis of the Legendre ellipse equivalent to the object (i.e., an ellipse with the same area, the first and second geometrical moments);
- dispersion DP ; obtained by Eq. (1.2), where P is the perimeter; A is the area of the particle

$$DP = P^2/4\pi A \quad (1.2)$$

- irregularity parameter IP , the ratio between minimum circumscribed and the maximum inscribed circles [16–23].

Based on the aspect of powder and structure characterization, the following important results of previous studies should be mentioned: powder granulometry is evaluated by means of the sieving analysis and image analysis depends on the distribution functions (count, length, area, volume or weight) and the image processing system (the measurement parameter of which is the basis of particle sizing). This is a very important result. It is the same structure analysis for example, when carbides on the structure have to be compared with the powder used or another system.

The disintegrator milling experiments of the production of ultrafine superalloy powders for binder metal of HVOF sprayed coatings also led to the problems of powder descriptions that mainly occur in lamellar forms [29].

The second important issue is now to select the parameters which describe morphology. It is necessary to determine preliminarily which shape differences should be covered. For this reason, it is impossible to recommend one or another characteristic as the best. The selection of optimum characteristics will always depend on real requirements. This is the main subject in the structure analysis, and selection of important structure parameters. It is also a good way of presenting relevant data.

To describe the microstructure of a powder and a coating it is necessary to choose parameters which describe the material in the best way. Previous studies of WC-Co composite powder and HVOFS coatings have demonstrated [24–28] that the use of recycled hardmetal powders in the formation of thermal spray coatings will lead to problems. Hardmetal powder particles sized from 30 to 40 μm in a thermal spray (detonation system, HVOFS) produce very porous (4 to 5 %) non-uniform coatings. Therefore, a new technology – mechanically activated synthesis [29] – was used to produce experimental WC-based composite spray powders. The new experimental powder allows for the enhancement of coating wear resistance.

To guarantee high abrasive wear resistance of a coating, it is necessary to optimize the structure of the coating. Thus, the choice of the method depends on the researcher. Commonly only SEM pictures and image analysis are used for

structure analysis, however, the distributions are mainly not shown that describe the distribution function used [30–35]. The main characteristic is the SEM picture of powder or coating to characterize them. The picture may not describe the overall material if the material is non-uniform.

For phase analysis, the XRD-analysis, a good method for phase analysis, is mainly used. Phase analysis is contradictory in W_2C and $Co_xW_yC_z$ phases. Rangswamy and Herman show that that it is not possible to form W_2C in the Co system [36]. But many of the authors have shown that after powder oxidation during the spraying process W_2C is formed in the W-Co-C system. The combustion process produces CO_2 and H_2O . The CO_2 and H_2O reaction with tungsten carbide is (Eqs. (1.3) and (1.4)) [37–38]:



The tests conducted with mechanically activated synthesis lacked the W_2C phase and CaO was the only oxidation product. But the difference may be caused by the composite powder production process.

As a result of wear resistance studies it has been concluded mainly that the nanostructured and the conventional coatings show approximately the same abrasive wear resistance, half of that obtained for the bimodal coating. The perfect mixture of the nano-sized carbides hardening the matrix and strongly fixed hard micron-sized WC grains seem to be the reason for the formation of a strong surface needed to enhance wear resistance.

From the abrasion test results it appears that the smaller the abrasive size, the better is the resistance of the coating to abrasive wear whatever its microstructure. But when the grain size of the abrasive is larger than that of the tungsten carbide particles, the role of the coating process that the coating structure depends on, is emphasized, and the HVOFS process will lead to improved abrasion resistance. In this case, the matrix (toughness, low porosity) and carbide properties (hardness, brittleness), the tungsten carbide–matrix interactions seem to play a major role in the cohesion of the structure as well as in its abrasion resistance [39–47]. Studies have shown that bimodal coatings are better than nanostructured or microstructured coatings. The carbide size distribution of the bimodal coating has not been reported to ensure the good wear resistance.

1.2 Safety belt tongue production and steel microstructure studies methods

The main terms of constructing technical delivery conditions in industry have been the quality requirements for the final product, production process requirements and *material price*. Cheaper or improper material can cause problems in production, starting with problems in fineblanking and ending with

those in heat treatment. This is why it is inevitable to know how the changes in THT affect the production process and what the possible limits of THT are.

Fineblanking material can be produced by different methods and it affects the material properties. Generally, material production consists of melting, hot and cold rolling, skin pass rolling, and soft annealing.

Melting process is important for steel cleanliness, chemical composition and structure. Most widely used steel melting processes for cold forming and fineblanking steels are the electric arc and basic oxygen furnace [78]. Calcium treatment is a step in secondary metallurgy to ensure steel cleanliness [63]. Inclusions formed by reactions are fine and globular and that type of inclusions is not elongated like MnS stringers. The globular type of inclusions is hard particles, not allowing deformation process in hot and cold rolling and therefore they can be abrasive to fineblanking tools. Even strong efforts and developments in the steel melting process do not lead to removal of non-metallic inclusions from steel and therefore it is necessary to observe them to establish the reasonable limits. *Casting process* can be continuous or block casting. In the casting process it is important to have a material without segregations. Alloying elements with carbon and sulphur appear mainly in the core region [78]. *Hot rolling* is used to reduce the thickness of the billets and provide the necessary structure of the material. Hot rolling starts with reheating to temperatures 1200 °C and 1350 °C throughout the cross section. The structure is controlled by controlling the temperature with the regulation of the rolling speed. There is a possibility to use thermo-mechanical rolling where the final rolling is made at the temperature according to the A_{c3} by Fe-Fe₃C phase diagram (austenite and ferrite area) [100]. *Cold rolling* is to achieve the good surface quality, high shape and flatness tolerances. The skin pass removes the flow platform in the tensile test, which is negative for tool lifetime. *Soft annealing* is the process used with carbon steels to obtain low strength values and high values of uniform and ultimate elongation. It is important to obtain a spheroidal carbide shape, which has a significant role in tool lifetime and cutting surface quality in fineblanking.

1.2.1 Production technology of safety belt tongues

Safety belt tongue production consists of three important steps: fineblanking, austempering and Ni-Cr coating by electroplating. Electroplating is followed by the baking process for hydrogen release.

Fineblanking was invented in Switzerland in the 1920s, fineblanking first attracted attention of manufacturers by combining stamping and shaving in one operation. This met requirements for dimensional accuracy, flatness and cut-edge quality without the need for secondary operations, such as grinding or machining. Besides advantages, the fineblanking material has strict requirements to the microstructure and chemical composition. Material microstructure is slightly described by the classical methods DIN 50601 and the spheroid carbides sizes and distribution by the standard SEP 1520 [79]. Modelling of the fineblanking process has been reported in many articles, however, information

about material properties is not available [79–83]. Good reviews of the deformations on the blanking process have been provided (Fig. 1.1).

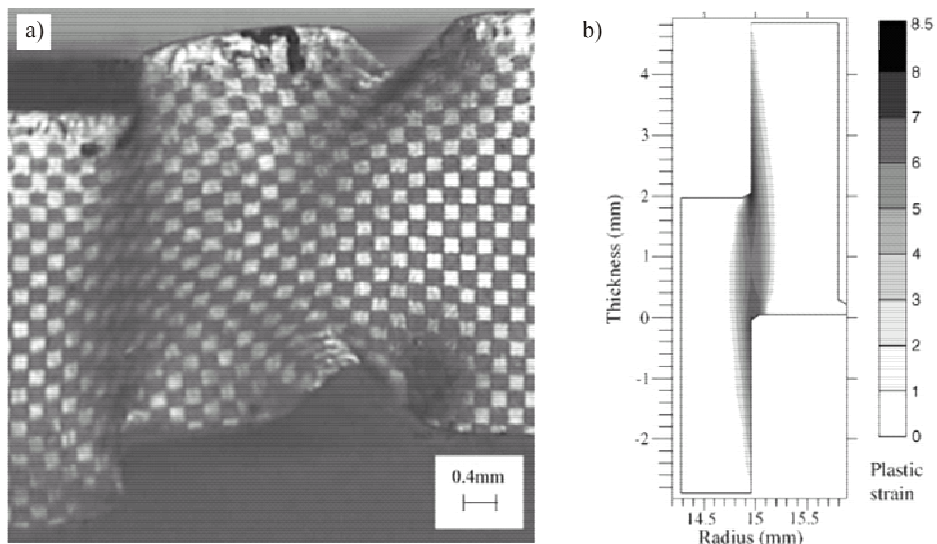


Figure 1.1 Fineblanking simulations (a) distorted mesh on the meridian plane of the fineblanked specimen and FEM prediction (b)

The tool consists of the elements shown in Fig. 1.2a. Figure 1.2b illustrates punch wear off cutting surface and the broken area (wear/fatigue). These problems may be caused by the blanking material.

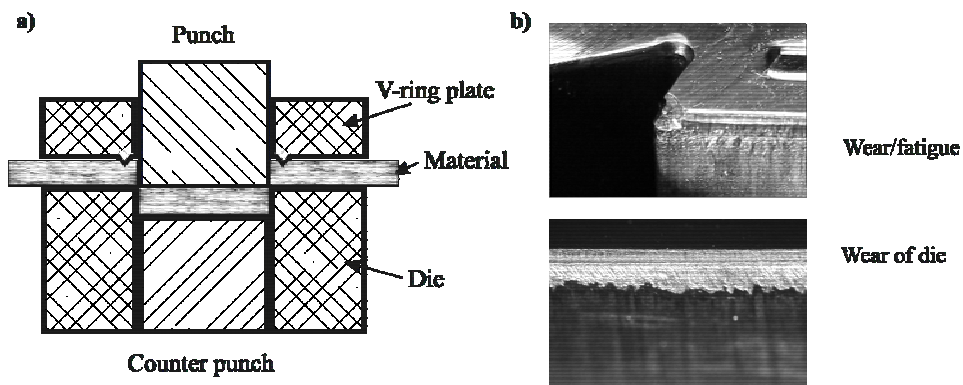


Figure 1.2 Fineblanking tool scheme (a) and die failure reasons (b)

Austempering is the second important process in the safety belt tongue production. Austempering with Ni-Cr electroplating makes the choice of the material even more complicated. In general, materials that are good in fineblanking are bad in heat treatment. The electroplating process is the third factor here, because hydrogen embrittlement is connected with heat treatment

structures [84]. Therefore, compromises between these processes have to be found.

Austempering is the isothermal transformation of a ferrous alloy at a temperature below that of pearlite formation and above that of martensite formation [85]. The structure obtained by the austempering process is bainite. The term bainite was first coined in 1934, in honour of Bain who reported this particular microstructure in 1933 [86]. There are different mechanisms and theories of bainite formation [86–91].

The factors affecting the austempering process are material chemical composition, austempering temperature and time, quenching speed, beinitization temperature and time, detail mass and geometry and austenite grain size [92–95]. The alloying elements, like Mn, Cr, Si and B, V, Nb, influence the austenite transformation speed and the shape of continuous cooling transformation (CCT) or time-temperature-transformation (TTT or C-curves) diagrams. Si, Al and Cu can lead to even bainitic transformation with phases retained austenite and ferrite. The larger austenite structure is supposed to reduce the austenite transformation speed [84]. The salt bath temperature and time are major components to regulate the structure and detail hardness – higher salt bath temperature ensures lower hardness, lower cooling speed of salt, and upper bainite [84, 89, 90].

Heat treatment line consists of the austenitization area (heating zone), cooling to the salt (bainitic transformation area) and the belt conveyer transport of the details to the water cleaning bath. The protective atmosphere is endothermic gas with a regulated carbon potential (CO and CO₂ percentages). The heating parameters are regulated with the required mechanical properties, material chemical composition, detail shape and size. Accurate regulation is performed through the Rockwell hardness measurements from the details on the production. Ni-Cr coating is an automatic process controlled by computer software. The coating chemical composition by EDS line scan is shown in Fig. 1.3. The main problem in the galvanization process is atomic hydrogen which diffuses to steel. The high strength structures are susceptible to the hydrogen embrittlement [96, 97]. The tensile strength of the safety belt tongue material after hardening is 1400–1700 N/mm². Hydrogen stress cracking (commonly known as hydrogen-induced cracking or static fatigue) is characterized by the brittle fracture of a typically ductile alloy under continued load in the presence of hydrogen. Generally, a fracture occurs at sustained loads lower than the yield strength of the alloy. This cracking mechanism, commonly considered a sub-critical crack growth mechanism that often produces time-delayed fractures, depends on the hydrogen fugacity, strength level of the material, heat treatment/microstructure, applied or residual stresses, and temperature. Several theories are available to explain the mechanism [97]. It has been found that the carbide/matrix interface is an effective, irreversible trap for hydrogen, capable of dramatically modifying hydrogen transport kinetics.

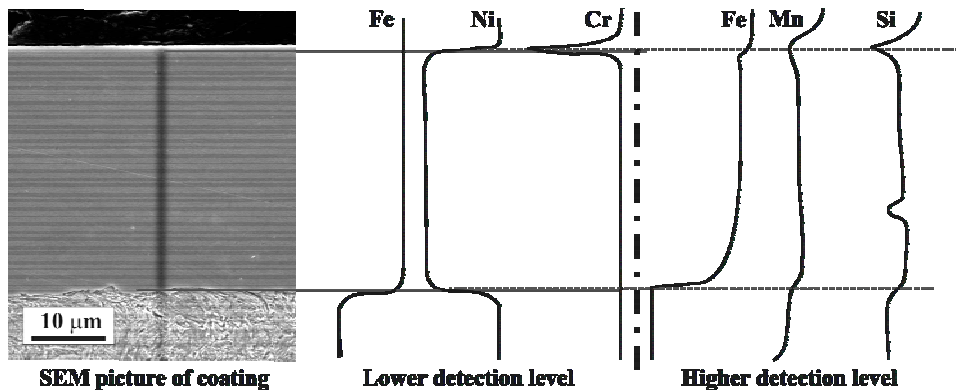


Figure 1.3 Ni-Cr coating line scan results on two different detection level

Some studies also demonstrate that carbides precipitate preferentially along grain boundaries and dislocations [99]. There are no studies which report relations between different bainitic structure and hydrogen embrittlement.

1.2.2 Microstructural evaluation of steel C60E

Many standard structure analyses are used to describe the steel microstructure methods [48–56]. Standard methods are mostly designed to analyze a material using a microscope and their use in computer analysis is complicated or even impossible. The example about classical method is the non-metallic inclusion analysis based on standard diagrams of DIN 50601 (Fig 1.4).

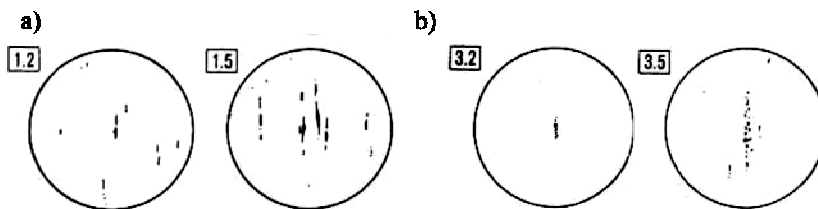


Figure 1.4 Standard diagrams of DIN 50601 (a) oxides and (b) sulphides

The new standards can be more suitable for computer analysis are for example EVS-ISO 84967:2005 because of shape and grain size analysis methods used with the same logic as required in computer analysis.

Non-metallic inclusions in steel can cause material defects on the exploitation and problems in production [57–61]. The inclusions are formed in the steel on the melting process. The type, appearance and chemical composition of these non-metallic inclusions can be very different and it depends on the factors, such as type of steel, melting process and the extent of shaping involved in obtaining the ingot or casting strand to a finished product [62–63].

The standard DIN 50602 is widely used in Europe to describe low alloy steel sheet metal cleanliness. There are several standards used for the same purpose.

This depends on the region where the steel producer or customers are situated. Other standards are ASTM E1245, E45, E1122, ISO 4967, DIN 50602, JIS G-555 and ГОСТ 1778. The standards can be totally different or vary from outputs, but these have practically the same methods to determine the non-metallic inclusions. There are several programs on the market, which calculate the non-metallic inclusions content by different methods. It is possible to use classical methods to obtain the non-metallic inclusions with computer analysis: stereological analysis, inclusions shape and colour; compare the standard diagrams with the help of a computer [64–72]. There are methods based other physical or chemical differences caused by inclusions: ultrasonic analysis, plasma spectrometric methods, SEM-EDS analysis [73–77].

1.3 Objectives and scientific novelty of the study

The main objective of this study is the development of structure analysis methods using a structure analysis computer programs. Modified structure analysis methods are for the determination of microstructure details affecting material properties that are not sensitive to conventional methods.

Based on the literature the following main tasks were set:

1. Developing methods for (a) describing granularity, morphology and the microstructure of composite powders, (b) evaluating the microstructure and composition of powder coatings produced by the HVOF spray technology and (c) clarifying the dependence of abrasive wear resistance of coatings on the structure.
2. To specify and develop the (a) structure analysis methods for low alloy steel C60E; to determine (b) the structure and chemical composition effect on the material behaviour during fineblanking and austempering and (c) to identify the factors that lead to hydrogen embrittlement.

The scientific novelty of this study consists in the following:

1. Specifying of the peculiarities of granularity and morphology analysis methods of composite powders produced by mechanical milling. Composite powders produced by mechanical milling methods. The coating bimodal microstructure was characterized with concrete numerical values.
2. The steel C60E was studied from the point of view of fineblanking, austempering and hydrogen embrittlement. During the studies new structure analysis methods for the low alloy steel C60E were developed to specify the carbides size and shape in the annealed condition.

2 EXPERIMENTAL

2.1 Powders and coatings

2.1.1 Composite powder production and particle size analysis

The WC-Co composite spray powder was produced using the mechanically activated synthesis (MAS). Tungsten was milled in the attritor milling system with carbon to the nanosize powder.

Nanosize was measured with the XRD crystal size analysis. The second option was an indirect method to analyze the powder surface area (Sorptometer KELVIN 1042 V3.06) and to calculate the average particle size [Paper II].

Activated tungsten and carbon were heated at the temperature 950 °C to obtain WC. Carbon content was measured by the Elementar Analysensysteme GmbH firm element analyzing system Vario EL V2.6.

WC mixed with Co was subsequently milled in the ball milling system for 24 h. Powder mixed with plastificator was sieved using a 63 µm sieve. The granules were sintered and the fraction of -45...+20 µm was used for spraying [Paper I].

To produce ultrafine powders by disintegrator milling (DM) with the particle size less than 5 µm, the DM system DSL-175 with the inertial and centrifugal classifiers was used. DM powders were milled in a protective environment – argon.

Disintegrator milled ultrafine metallic powders were characterized by the following methods [Paper III]:

- specific surface area measurement;
- particle size analysis;
- oxygen content measurement.

Table 2.1. Investigated powders

Powder index	Powder type	Powder size
3-6	Mechanically activated W-C nanopowder	30 nm
3-7	WC obtained from MAS	130 nm
MAS	WC-Co composite spray powder	20 – 45 µm
Anval-Ultimet	DM milled Co-alloy powder	1 – 5 µm

The granule size and distribution in the powders studied were examined with the help of three analysis methods:

- sieve analysis (-45 ... +20 µm);
- laser diffraction analysis by Laser particle sizer Analysette 22 Compact;
- image analysis based on the Image-Pro Plus 3.0 system (IPS) and Omnimet image analysis system 4.1 (OMS).

2.1.2 Thermal spraying of coating

The HVOF spraying system TAFA JP 5000 (Praxair Tafa, USA) with kerosene as a fuel was used to deposit the coating. Spray parameters applied to spray the coating are shown in Table 2.2.

Table 2.2 Spray parameters for the HVOFS system

Parameters	TAFA JP 5000	
Fuel and gases flow, l/min	Kerosene	0.38
	Oxygen	1066
Fuel and gas pressure, kPa	Kerosene	828
	Oxygen	938
Deposition rate, kg/h	9.0	
Spray distance, mm	380	

The coatings (Table 2.3) were deposited on the carbon steel plates (0.45 % C) as a substrate material. The plates had the length, width and thickness of 60 mm, 35 mm and 10 mm, respectively. Coating thickness after spraying was ~ 300 μm .

Table 2.3. Investigated coatings, spray powders, and the indexing system

Coating index	Type of coating	Powder (μm)
A	(WC-Co)-15Co (experimental, agglomerated)	15 – 45
B	WC-17Co (TAFA 1343 V) (commercial)	20 – 50
C	WC-15Co (mechanically activated synthesis)	20 – 45

2.2 Steel C60E

The development the technical delivery conditions for steel is a process that involves both the users and the producers of the material. *AS Norma* suppliers are mostly German steel companies, occasionally also Russian and Czech companies. The C60E material is from Germany, because the trials from Russia were poor in quality. Co-operation with suppliers was based on the negotiations about the requirements to the mechanical, chemical, structural, and dimensional properties of steel, which served as a basis for the development of the THT requirements Table 2.4.

Table 2.4 Material types ordered form the suppliers

Steel	C	Si	Mn	P	S	Cr	Cu	Mo	Ni	Al
65G*	0.66	0.29	0.98	0.019	0.004	0.01	0.04	0.01	0.02	0.039
Low Mn	0.60	0.10	0.36	0.005	0.001	0.25	0.06	0.02	0.06	0.023
TH I	0.60	0.22	0.02	0.007	0.003	0.24	0.06	0.02	0.05	0.007
TH II	0.60	0.22	0.02	0.007	0.003	0.24	0.06	0.02	0.05	0.007
Type II	0.59	0.24	0.64	0.010	0.001	0.22	0.02	0.02	0.05	0.007
Type II	0.60	0.19	0.73	0.015	0.001	0.26	0.03	0.01	0.05	0.020

* Material with 70 % spheroidal structure.

2.3 Methods for structure, chemical composition, and phase analysis

Preparation of cross-section polishes for structure analysis for powder, WC-Co coating and steel was carried out in different ways.

For particle structure and composition analysis, cross-section polishes were made by the mechanical grinding-polishing procedure. The best results were obtained by a fluid (not viscous) cold mounting by an epoxy-based compound. The powder was mounted by the help of the Buehler vacuum impregnation system. Due to the high hardness of WC particles, diamond grinding-polishing was used.

For coating analyses, hot mounting was used because it has higher hardness than cold mounted epoxy-based compounds. Higher hardness ensures the planarity of a specimen. Different methods were used for grinding and polishing.

Hot mounting with Epomet powder by Buehler was used for steel specimens. As steel is softer than a WC-Co material it is not easy to obtain a good polished surface and non-metallic inclusions without artefacts. The corrosion problem of steel inclusions was as special problem, therefore water was not used in the final steps.

The chemical composition of the structure elements was studied by means of the energy dispersive X-ray microanalysis (EDS) with the Link Analytical AN10000 system. The X-ray mapping technique was used to evaluate element distribution inside powder particles. According to the results, the resolution of element distribution is 0.5 to 1 μm . The chemical composition of steel was analyzed by the spark analyzer Spectrolab M, produced to analyze the chemical composition of the construction material on the basis of Fe, Cu and Al [102].

The microstructure was investigated by means of the optical microscope Axiovert 25 and scanning electron microscope (SEM) Jeol JSM-840A, using backscattered and secondary electron imaging. Quantitative results of the structure analysis were obtained by the image analysis systems OMS and IPS.

To describe grains and powder granule shape, the following parameters were used: *dispersion DP* is defined as the ratio of the convex perimeter to the perimeter (if there is no concavity at the edge of the particle, the roughness of this particle is 1.0); *roundness RN* is defined as $4\pi \cdot \text{area} / (\text{perimeter squared})$ (if the shape of the particle is a perfect circle, the *RN* of this particle is 1); *aspect ratio AS* refers to the longest axis of the observed object, divided by the shortest axis of the same object.

The phase composition study of the investigated samples was carried out on the Bruker D5005 X-ray diffractometer (XRD), using Cu K α radiation at 40 KV and 40 mA. The range was 11–70° by step 0.040° and step time was three seconds.

For the *steel structure analysis* methods, international standards were used. Non-metallic inclusion analyses were carried out by the German standard DIN 50602 [48]. To obtain cleanness M and K methods are widely used. M method is easier to obtain but it gives information about the largest non-metallic inclusions. To acquire a full description of inclusion it is necessary to measure both methods. It is difficult to measure by the K method, particularly in the case of unclean steels,

but the K method helps to determine the quantity of sulphides and oxides to 1000 mm² Eq. (2.1).

$$K = \frac{\left(\sum_{g=0}^8 n_g \cdot f_g \right) \cdot 1000}{A} \quad (2.1)$$

K is the content of non-metallic inclusions, n_g is the number of fields according to the rating ($n = 8$ classes), $f_g = 2^{n-4}$ is the weighting index and A is the investigated area. Rating classes can be obtained from standard diagram, showed on Fig. 1.4. K1 and K4 method differs from each other detection level. K1 method counts fields from first class and K4 from forth class. The M method shows the highest rating class obtained from material analysis.

Spheroid carbides are determined visually by the help of the standard SEP 1520 “Microscopic examination of carbide structure in steels by means of diagram series”, which serves as a basis for steel manufacturers in Germany [50].

Austenite and ferrite grain size was determined according to DIN 50601 by a comparison method or by computer analysis (OM). The austenite grain size was determined by heating the sample up to 850 °C in protective environment, holding 20 min and oxidizing in air which is described in the EN ISO 643:2003. Grain size was calculated according to ASTM E-112 when obtained by DIN 50601 [51, 53].

Surface decarburization was measured according to the standard EN ISO 3887:2004 [54]. The determination of surface decarburization was based on visual examination or hardness measurements. According to the standard, different measures are possible: total surface decarburization and partial surface decarburization.

2.4 Methods for mechanical testing

2.4.1 Tensile and bend tests

Main mechanical requirements to the safety belt are tensile strength and toughness.

Bending test is to control hydrogen embrittlement after galvanization. Before the galvanization the material did not have brittleness. Bending test was performed by the scheme shown in Fig. 2.1a. From one production batch, 10 safety belt tongues were tested. All the tongues have to withstand the bending angle over 30 degrees. Tensile tests were carried out with safety belt tongues using the method shown in Fig. 2.1b. Like with the bending test, 10 details from one batch were tested. The testing was carried out after heat treatment, galvanization and overmoulding.

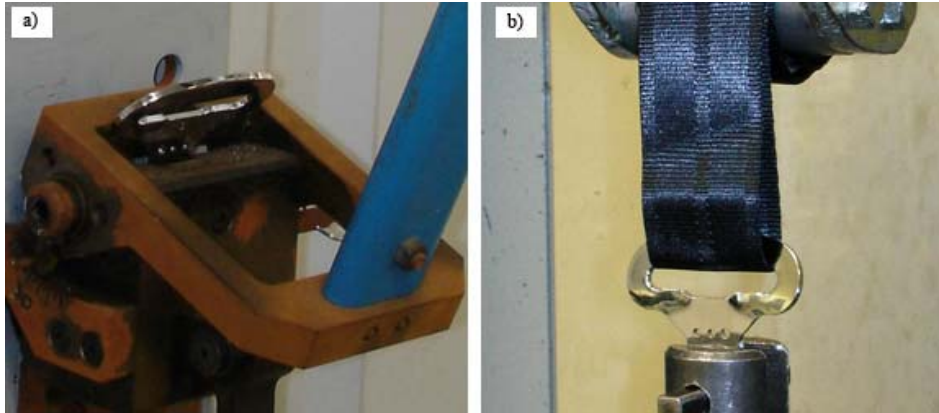


Figure 2.1 Methods for testing tongues: (a) bending test and (b) tensile test

Tensile test requirements of the safety belt tongues differ by the type of tongues, but the minimum allowed value mainly is 23000 N minus 3 or 6 sigma Eq. (2.2) requirement.

$$23000 < EX - 3 \frac{\sum_{i=1}^n |x_i - EX|}{n} \quad (2.2)$$

Therefore it is important to have not only high values but also equal values of the tensile test to accomplish the 3 or 6 sigma requirement.

The standard test of the safety belt material, the tensile test according to EN 10002-1 and Instron 8516, was used [101]. Test specimen width in the annealed conditions was 20 mm and values R_m , $R_{p0.2}$, A_{80} , A_g are important in the annealed condition.

To analyse material hardenability, special specimens were worked out where the width is decreased to 8.5 mm (like that of the broken area of the safety belt tongue). The specimens made of different materials were austempered at the same condition or with different heat treatment parameters (depending on the purpose). Heat treated specimens were tested to the tensile properties and after Rockwell hardness tests from the middle area (8.5 mm width) and from the specimen grip area (32 mm width). Differences in Rockwell hardness show the hardenability of the material with R_m values and the difference in Rockwell hardness from the middle and centre area.

2.4.2 Wear resistance testing

The dry abrasive wear resistance test was performed according to ASTM G65–94 [105]. Abrasive – quartz sand with particle size 0.1-0.3 mm was used. The amount of sand was 3.0 kg; disc diameter was 228.6 mm, the speed was 2.4 m/s, distance 1440 m, and force 222 N.

3 RESULTS AND DISCUSSION

3.1 Characterization of powders and coatings

3.1.1 Granularity and morphology of initial and spray powder

To produce composite powders with sub-micrometric WC grains, an analysis of a sub-micrometric powder by indirect methods, like BET or XRD, was carried out to measure the WC powder [Paper II].

The BET method enables us to find the surface area S and then calculate the average particle size Eq. (3.1), where ρ is the density of material (WC $\rho=15.72$ g/mm³); Dv is the average grain size diameter on micrometers by volume.

$$Dv = \frac{6}{s\rho} \quad (3.1)$$

The size analysis results of nano powders are shown in Fig. 3.1, where powder 3-6 is W and C powder in an activated phase and powder 3-7 after heating of the WC phase. In Fig. 3.1, d_{50} is grain size at 50 % frequency, EX is the arithmetic mean value Eq. (3.2).

$$EX = \frac{\sum_{i=1}^n x_i f_i}{\sum_{i=1}^n f_i} \quad (3.2)$$

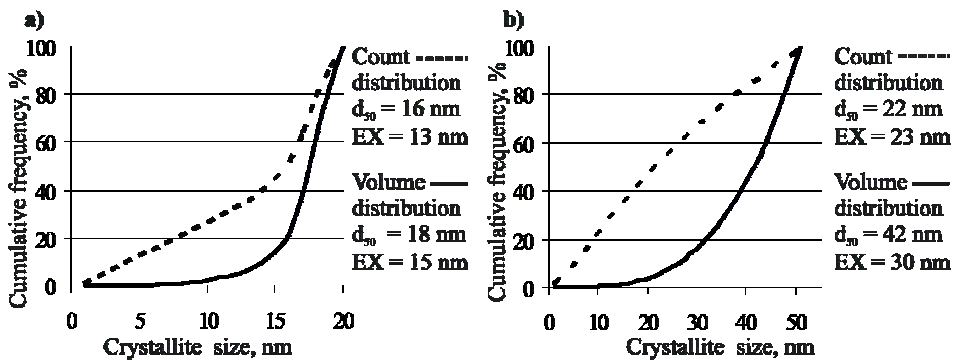


Figure 3.1 Results of XRD crystallite size analysis by the BET analysis: a – Powder 3-6, $Dv=30$ nm and b – Powder 3-7, $Dv=130$ nm

There are differences in the crystallite size of the powder in the activated phase and heated because a particle consists of more than one crystallite. The differences are increasing as the particle size is growing. The average diameter

calculated from the surface area is comparable with the volume distribution values because the calculation by Eq. (3.1) is based on the volume of the particle.

Figure 3.2a shows the SEM picture of the composite granule and Fig. 3.2b shows the sub-microstructure of final granules, the size of which can be analyzed in high magnification with the image analysis systems. This particle size remains in the coating structure with no noticeable growing.

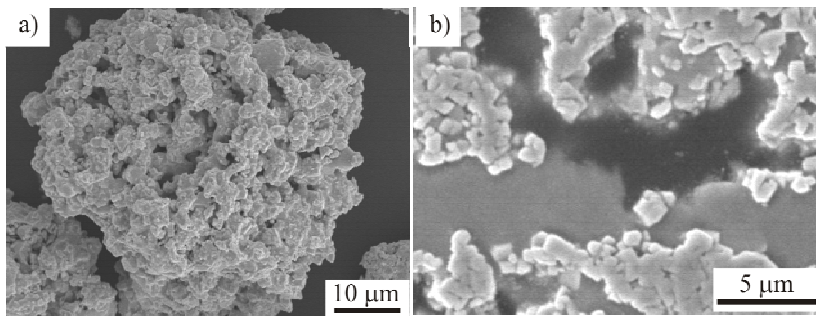


Figure 3.2 SEM micrographs of powder granule C: a – granule, b – granules cross-section

For thermal spray, the granule size of the powder should range from 20 to 45 μm to achieve high productivity of spraying and avoid oxidation processes. It is much easier to determine the particle size and size distribution of composite powder granules than WC nanoparticles because of their larger size. For the granulometry studies the analysis of image, sieve and laser particle size can be used. Sieve and laser analysis may yield different results because of the elongation of the granules (Fig. 3.3). Aspect ratio AS was used to characterize their elongation. The mean aspect ratio was 1.96, which means that the longest diagonal of the particle is almost twice as long as the smallest one (Fig. 3.3a and b). Because of such an elongation, the values for the granule size measured by a laser diffraction analyzer were larger than 45 μm (the largest by sieving).

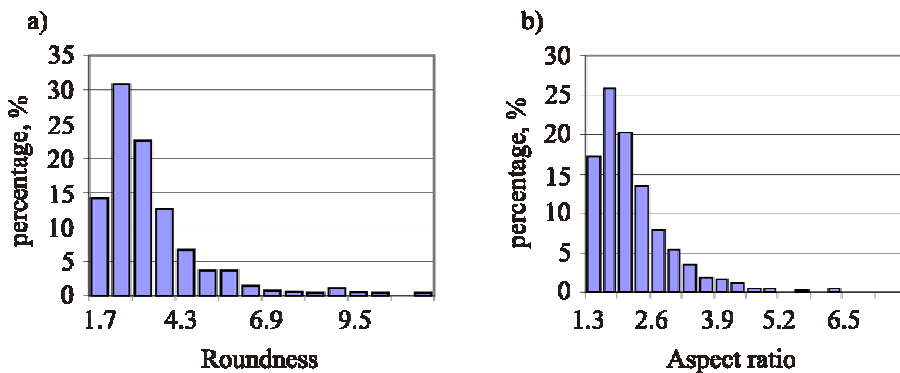


Figure 3.3 Results of granules shape analyses: a – roundness RN and b – aspect ratio AS

In the laser analysis, 28 % of the granules measured were over 50 μm in size and 5 % were less than 20 μm (smallest by sieving). Granules over 45 μm can go through the sieve because of their elongated shape [Paper I].

The results of the image analysis using the *IPS* system for granule size were similar to those of the laser analysis (Figs. 3.4a and 3.4b). For the image analysis, it is necessary to do powder cross-section polishes and pictures. On the image analysis pictures, granules have to be cleaned and separated from each other, therefore it is easier to perform laser and sieve analysis. The pictures can be used to control the results, especially in cases where the analysis results are somewhat incorrect.

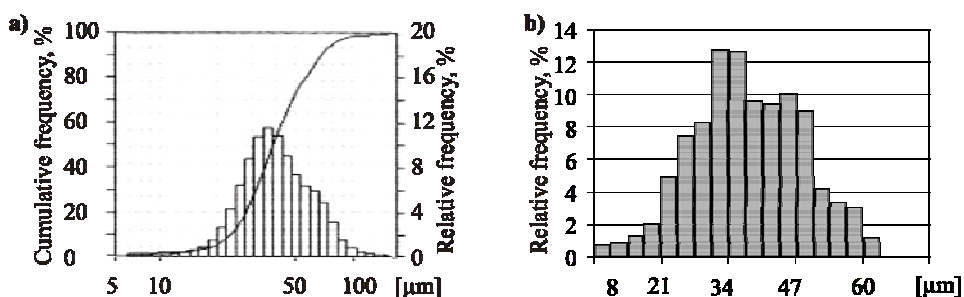


Figure 3.4 Powder C granules volume distribution using: a – measured by laser particle analyzer, b – image analysis

Indirect methods do not suit for the analysis of composite powder granule sizes. XRD can provide the size of WC crystals. The BET analyses indicated a larger surface area because of open porosity (Fig. 3.3a and b). The open porosity can be described with the shape parameter *DP* and it is important when spraying and when granules oxidation occurs.

To produce an of experimental spray powder, the agglomeration of ultrafine powders (particle size in the range of some μm), commercial WC powder and Co-alloy powder produced by high energy *DM* were used. Figure 3.5 shows the particle shape of the milled powder and Fig. 3.6 present the particle size distribution by volume determined by the laser particle size analyser and image analysis.

As it follows from Fig. 3.5 the disintegrator milling of ductile material as Anval-Ultimet produces coarser spherical and finer plate-form particle micropowders. Most of the powder particles had a relatively large elongation (mainly close to 2), which is normal in grinding of ductile materials by collision in the disintegrator mill [Paper III]. According to the results presented in the Fig. 3.6, the image and laser analyses show similar results.

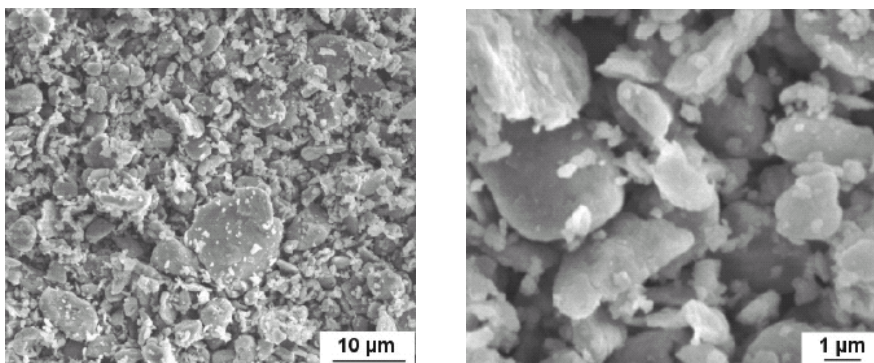


Figure 3.5 SEM images of ultrafine powder Anval-Ultimet

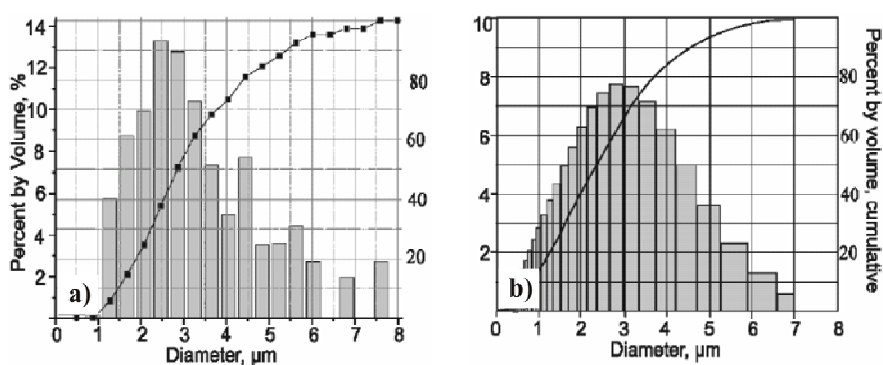


Figure 3.6 Particle size distribution of ultrafine powder Anval-Ultimet: a – image analysis, b – laser analysis

Regardless of DM milling in the protective environment, i.e. argon, due to a very high specific area of the powder Ultimet after milling, the oxygen content of the powder increased catastrophically both at milling and during its handling in the air. This is in direct correlation with the increase in the specific surface area of the powder (Table 3.1).

Table 3.1 Specific surface area and O₂ content of the initial and milled powders

Powder type	Initial		After milling	
	Specific surface area, m ² /g	O ₂ content, %	Specific surface area, m ² /g	O ₂ content, %
Alloy-Ultimet	0.044	0.13	3.42	11.7

To decrease the O₂ content, the annealing of powder in hydrogen at temperatures 650, 850 and 1000 °C was conducted. The decrease in O₂ content was only 5-20 %.

The spray granules were made from Alloy-Ultimet using agglomeration-sintering technique. The granules size was 20-45 μm and according the production method shape were spherical.

3.1.2 Phase analysis of powders and coatings

The most effective and easiest way to analyze powder or coating phases is the XRD analysis. WC-Co granules and coatings mainly have two phases (WC and pure Co), and the phase composition can be studied by XRD, SEM photos and by X-ray mapping. According to the XRD analysis, powder granules have the following additional phases: W and $\text{Co}_3\text{W}_3\text{C}$. The coating has the same phases, except that CoO appears as a result of oxidation during the spraying process [38]. The XRD analysis does not show the Co-phase because the XRD Cu-cathode radiation diffuses in the Co crystal lattice [2]. SEM photographs, X-ray mapping and hardness testing confirm that pure Co is one phase. $\text{Co}_3\text{W}_3\text{C}$ is formed because of the low carbon content (4 %) in the powder (less than 6.1 %) [103]. W_2C can not form because of Co and forms $\text{Co}_x\text{W}_y\text{C}$ phases in the structure which are darker under the SEM than WC [36].

SEM picture phase tones (W and Co have different tones under SEM because their atoms have different masses) can be the bases to obtain the phase content by computer. SEM photos can provide more information for the exact phase analysis because resolution and contrast is higher than in X-ray mapping [Paper I]. Figure 3.7 shows the phases obtained during the SEM investigations. From these areas, quantitative EDS analysis was made (area was too small, phases under and near affect the analysis). WC coating structure component consists probably of the WC and Co phase which have a eutectic form, which can be the result of high cooling speed (Fig. 3.7a upper right area).

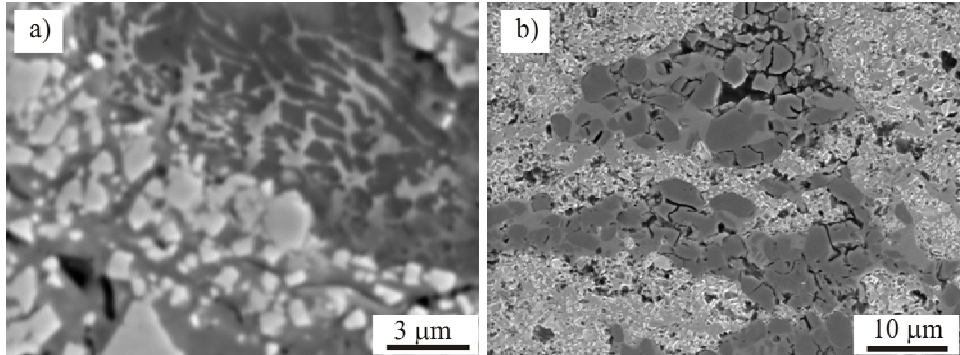


Figure 3.7 SEM pictures of WC-Co coating: a – eutectic phase and b – $\text{Co}_3\text{W}_3\text{C}$ phase

$\text{Co}_3\text{W}_6\text{C}_2$ has lower mass than WC, therefore it is darker on the SEM images and can be seen in Fig. 3.7b. The material between $\text{Co}_3\text{W}_6\text{C}_2$ can be the tungsten solid solution in the cobalt matrix. Solid solutions in the material are underestimated and it is hard to analyse them on the basis of SEM pictures, neither does XRD show a solid solution. Sometimes the SEM pictures contain different tones of the same phases that may be caused by the solid solution.

3.1.3 Microstructure and porosity analysis of coatings

Microstructure and porosity analysis starts from accurate preparation. For coating it is necessary to achieve a good edge quality specimen. Therefore, right methods of mounting, grinding and polishing are necessary. The surface is required to be flat (not relief), with minimum deformations and corrosion. The structure of the prepared specimen has to reflect the real material structure. Thereby several tests with different methods were done and preparation effect to porosity was studied.

For computer analysis the most important step is to recognize the phases or porosity and their shape based on the tones and pixels combinations. It has to be done with accurately measured magnification and pictures with possibly the same contrast. Figure 3.8a shows a SEM picture of the coating and Fig. 3.8b shows the picture cleaned by hand and clear for computer analysis. Cleaning with hand is a very labour-intensive process, therefore automatic computer recognition is used [Paper II].

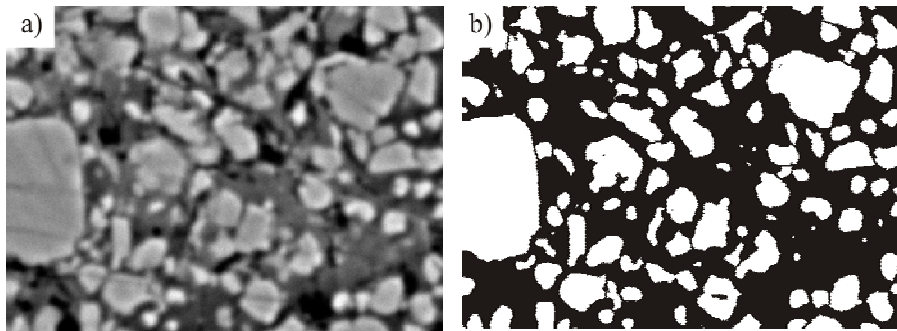


Figure 3.8 WC grains for the computer analysis: a – SEM picture and b – treated picture

For that purpose it is necessary to make the routine (program inside OMS). The effectiveness of the program for structure analysis is dependent on the routine. Computer phase analysis with the automatic phase detection can be accurate, as shown in Table 3.1. In the Table 3.1 OMS is automatic phase detection, OMS BW is manually cleaned pictures of phase detection and IPS BW is analysis based exactly on the same pictures as OMS BW [Paper II]. However, even by the same methods and same clearly cleaned BW pictures, the values can differ, as shown in Table 3.1.

Table 3.1 Comparison of different methods (magnification 2K-2000X and 5K -5000x)

Measured values	OMS 2K	OMS BW 2K	IPS BW 2K	OMS 5K	OMS BW 5K	IPS BW 5K
Ferret, Avg, μm	0.8	0.7	0.7	0.8	0.6	0.7
Aspect AS	1.5	1.6	1.7	1.5	1.6	1.7
Roundness RN	0.6	0.7	0.8	0.5	0.7	0.7
WC, %	38.2	41.6	40.1	44.3	39.9	41.1

The database cannot consist only of the pictured fields of the same area. The area investigated should be large. In most cases, the area of a sample is rather limited and therefore studies are based on a limited area. However, this does not mean that the test area has the same structure with all other materials, in particular when analyzing the material structure with high magnification, where one field is very small. Therefore real-time computer analysis with automatic phase detection is the best solution.

The porosity measurement method description is shown in Paper II. In the porosity analysis it is very important to choose the right microscope (the results of the light optical microscope analysis are more reliable than those based on the SEM pictures) and an operator with adequate experience. Different operators measure porosity differently and systematic errors from equipment have a relatively small effect. Therefore, it is necessary to use equal methods for comparison of different materials parameters. Figure 3.9 shows the results of porosity analysis in different fields. The different fields were obtained by grinding a new metallographic plane, followed by porosity analyses. The coating C porosity varied from 0.2 to 2.8 % on the different area. Even when the magnification is relatively low (500X), the structure of material is not homogeneous.

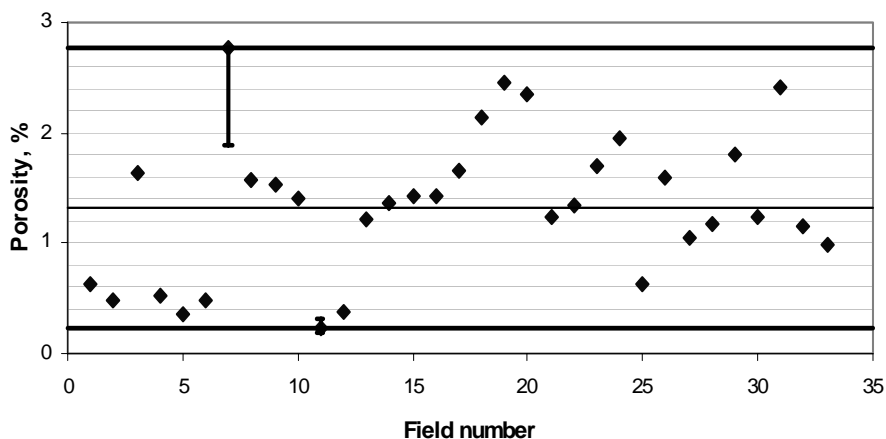


Figure 3.9 Coating porosity analysis in different fields

In Fig. 3.9 the accuracy of the analysis is estimated, vertical lines on the upper and minimum level show the measurement accuracy. It shows the deviation of picture calibration and calibration etalon, operator accuracy with threshold levelling and microscope lighting range.

Average grain size diameter can be different, depending on the method of measurement, on the method of calculation and most importantly on the distribution (count, length, volume or weight distribution). It is not easy to show the results of structure analysis where structural differences are clear. Table 3.2

shows the results of structure analysis and Fig. 3.10 shows coating structures B and C.

Table 3.2. Results of structure analysis by the OM analysis

Parameters	Coating A	Coating B	Coating C
WC phase, %	38.2	48.5	44.4
Co matrix, %	42.5	49.2	51.9
Porosity, %	3.7	1.1	1.3
Dv, μm	1.2	1.8	1.1
Dc, μm	0.7	0.8	0.8
Roundness <i>RN</i>	0.6	0.6	0.6

The structures are visually different, Table 3.2 shows that there is no difference on the spherical mean diameter (calculation based on the count distribution). At the same time, mean diameter by volume is different and it differs more than twice with the structure. Thus to show a more fine grained structure, count distribution should be used.

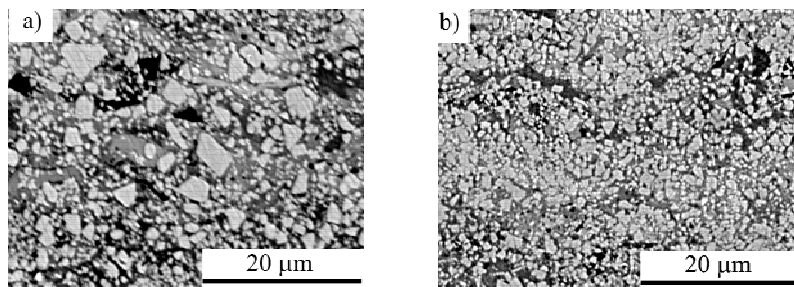


Figure 3.10 SEM pictures of coatings structures: a – coating B and b – coating C

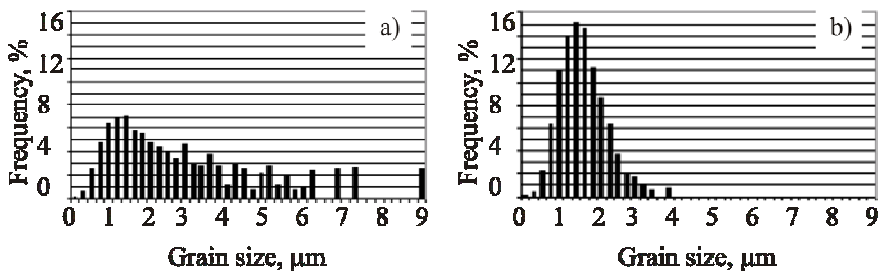


Figure 3.11 Volume distributions of WC: a – coating B and b – coating C

The main microstructure (WC-Co) characteristics that have an effect on the abrasive wear resistance of the coating are as follows: porosity, grain size, and size volume distribution [104].

Figure 3.11 shows the WC size of volume distribution. The size of volume distribution is calculated on the basis of spherical diameter, which is the OMS system calculated from the measured grain surface area S Eq. (3.3).

$$D = 1.22474 \sqrt{\frac{4S}{\pi}} \quad (3.3)$$

Structure analysis programs give discrete statistical values where each class of average size has a certain frequency. It is count distribution, where particles are counted to the classes (i to n) and each class (x particles) has a certain percent f_{ic} to the overall amount (all particles count N in Eq. (3.4)).

$$f_{ic} = \frac{x}{N} 100 \quad (3.4)$$

For volume distribution it is necessary to calculate average particle volume V_i based on the class average diameter D_i for each class Eq. (3.5).

$$V_i = \frac{4}{3} \pi D_i^3 \quad (3.5)$$

$$f_{iv} = \frac{V_i f(\mu m)_{ic}}{\sum_{i=1}^n V_i f(\mu m)_{ic}} 100\% \quad (3.6)$$

The volume distribution, which is expressed on average particle diameters D_i is the calculated frequency f_{iv} of each class of particles volume to the overall particle volume Eq. (3.6). Volume distribution emphasizes large particles and is the same distribution with sieve analysis (weigh distribution) and laser particle analyzer analysis (calculated volume distribution).

Count size distribution does not show larger grains in the distribution at all. Therefore particle size distribution by their volume is a better indicator showing differences between the structures based on larger grains (Figs. 3.10 and 3.11).

Differences in volume distributions are clearly visible. Coating C has high wear resistance because of the small and homogeneously distributed grains [Paper II]. In WC grain size distribution, the main mode is at 0.9 μm and the other at 2.2 μm . Despite the smaller porosity of coating B (compared to coating C), wear resistance is not so good because the average size of larger particles is 5 μm , although the average size of small grains is the same – 0.9 μm . It means that in coating C, grain size differences between large and small particles are smaller. The structure of coating A has approximately the same distribution of small and larger particles as coating C but its porosity is three times higher (Table 3.2) and

therefore the wear resistance is low. Relative wear resistance of the investigated coatings is presented in Table 3.3.

Table 3.3. Relative wear resistance of coatings

Coating index	Type of coating	Relative wear resistance
A	(WC-Co)-15Co (experimental, agglomerated)	5.3
B	WC-17Co (TAFA 1343 V) (commercial)	10.3
C	WC-15Co (mechanically activated synthesis)	23.2

Based on the experiments and microstructure analysis, dry abrasive wear resistance of the WC-Co coatings depends mainly on the porosity, carbide content in the coating and volume size distribution. Other investigated parameters had a minor effect on the wear resistance.

The following conclusions from this part may be drawn:

- Crystallite size analyses fail to give an accurate nano-powder size because nano-particle consists of more than one crystallite.
- For characterization of micro-powders size as the image and laser particle size analysis should be used, where laser analysis are most effective.
- To characterize the composite powder granules, volume distribution should be used and additionally shape parameters should be analyzed, in particular when the results of sieve analysis and laser analysis are different.
- To describe the porosity and particle irregularity, it is useful to combine different methods, BET method (irregularity), image analysis (closed porosity), and laser analysis for granule size.
- To analyze macro-, micro-, and sub-microstructures, it is possible to make an effective use of classical methods, for example when analyzing phase and elemental weight composition on the basis of SEM photos.
- To characterize the microstructure and sub-microstructure of composite powder granules, agreed numerical values (size distribution, average values and shape parameters) are needed, so that they could be compared with the results of other experiments.
- Computer corrected pictures and hand corrected can be of the same quality, but the correction program and results have to be controlled. For a good computer structure analysis, it is very important to have metallographic preparation of high quality.
- To obtain average numerical values of the microstructure and porosity, it is necessary to examine more fields (15 to 20 fields, depending on the homogeneity of the coating structure).
- Grain size distribution by count is not sensitive to the changes in the microstructure; therefore, in order to obtain useful information, grain size distribution by volume must be used.

- Microstructure analyses of coatings enable us to show that one particular WC particle volume distribution: uniform distribution of small-size hard particles (about 1 μm) and a certain amount (5 to 10 % by volume) of larger hard particles (2 to 3 μm) is one of the main reasons of good dry abrasive wear resistance.

3.2 Structural aspects of the Ni-Cr coated steel in the production of safety belt tongues

3.2.1 Describing of steel C60E structure at the annealed condition

A need for computer structure analysis was derived from previous testing where the standard test failed to explain materials properties differences. The structure analysis studies were made with a complex analysis of the material starting with the effect of chemical composition on austempering and ending with the relations of mechanical properties to the microstructure.

The chemical composition of safety belt steels influences mainly the three aspects of safety belt tongue manufacturing: tool lifetime, hardenability and hydrogen embrittlement of the detail. From the metallurgical point of view, the chemical content is important to steel manufacturers. Changing the chemical content of the material is complicated because the evaluation of the effect of the change on the properties is very complicated for any given specialist. The material technical delivery condition (THT) worked out in order to achieve a suitable material for safety belt production.

Minor changes in the C60E chemical composition and structure can affect the steel hardenability because of slow quenching salt's cooling rate. Figure 3.12 shows the dependence of the tensile strength of hardened specimens on the content of Mn. The effect of other chemical elements is not so distinct. Test specimens width 8.5 mm was austenized on a continuous line at 850 °C for 28 min and then quenched to salt bath at 325 °C for 8 min. *Material with 0.71 % Mn (Type II) compared to material with 0.64 % Mn (Type I) had systematically worse hardenability, which was the reason to find differences from the structure [Paper IV].* Material with lowered Mn content 0.36 % was not suitable for tongue production. It is possible to achieve correct hardness in the controlling spot, but at the same time other problems occur, like the wider tensile strength deviations of the safety-belt tongues (lower strength characteristics) and high hardness differences. Hardness differences are measured from the tensile test specimen centre and grip area. It is interesting that hardness and tensile strength are not exactly in correlation, higher Mn content (without structure differences) results in higher tensile strength test with the same hardness (Fig. 3.12).

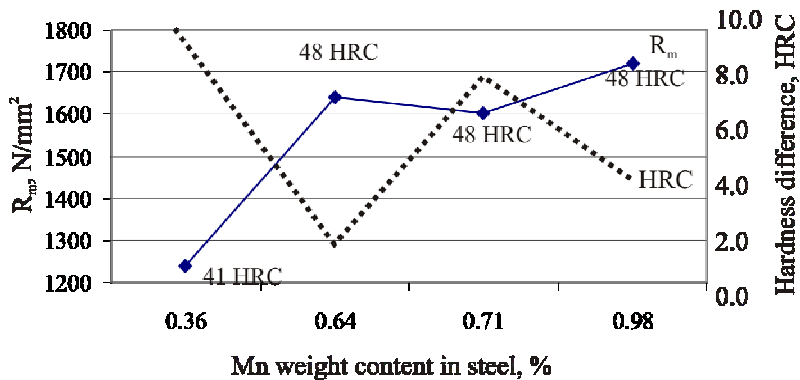


Figure 3.12 The effect of Mn on tensile strength and hardness

Therefore, at THT 031 issue 4 Mn content is increased to ensure hardenability. At THT 031 issue 5, the upper limit of Mn content lowered again and we narrowed the limits of C and Cr. It is inevitable to keep the content of Mn in an optimal range, because increasing the Mn content means a too high increase in the strength characteristics in the annealed condition. Tighter limits of C and Cr keep the mechanical characteristics of the material more sustained, leading to a more sustained production process (the geometry changes of the cutting-elements of the stamping tool, parameters in heat treatment). Alloying with Cr is one of the ways to increase the hardenability, however it is not economically reasonable.

Tensile strength and hardness were not the only parameters that the material composition affected. Problems started with details made from lowered Mn (0.36 wt. %) content and type II material in the electroplating, with hydrogen embrittlement. It was not a logical outcome, i.e., a softer material having more problems than a harder one (Fig. 3.13).

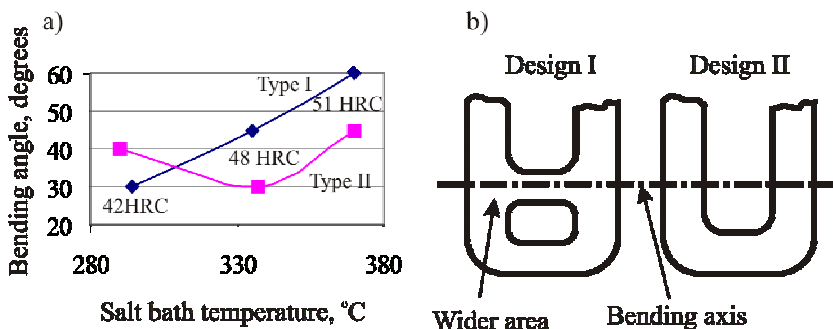


Figure 3.13 Bending tests to analyze hydrogen embrittlement

Electroplating as a reason was excluded in several tests in heat treatment line which showed systematical dependence on the material or heat treatment

parameters (Fig. 3.13a). Tests were carried out with design I safety belt tongues. It was interesting that with design II tongues made from type II material no problems with hydrogen embrittlement occurred. Thus, a proof was provided with material hardenability (on the bending line design I has a wider area, Fig. 3.13b). The same is shown by the measurement of hardness difference (Fig. 3.12).

It was possible to explain hydrogen embrittlement in lower hardness by the hardened structure analysis. Figure 3.14 shows two cooling curves (v_1 at lower salt temperature and v_2 at higher salt temperature) and two different types of material C-curves (type I and type II). A wider part of the material cools down at a slower velocity (Fig. 3.13b design I). Material type I used with the design I tongue has a wider part in the bending area. The material cools down there according to the cooling curve v_1 (Fig. 3.14) and the structure consists of upper bainite (Fig. 3.14a). Material Type II C-curves are more right or using design II safety belt tongue, the cooling velocity is higher and in the microstructure, the main component is the lower bainite (Fig. 3.14b). The upper bainite or thin long parallel carbides are susceptible to the hydrogen content in the material and therefore safety belt tongues are more brittle than with the higher hardness lower bainite.

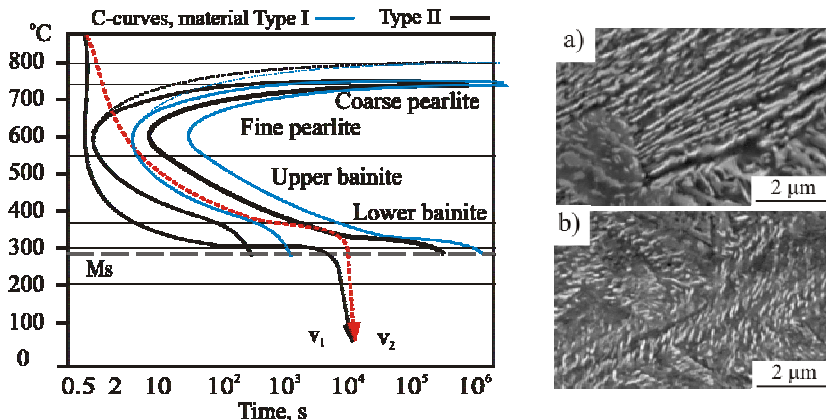


Figure 3.14 C60E CCD-diagram with SEM pictures about the austempered C60E type

At the lower temperature of salt bath, cooling velocity in salt is higher and the cooling curve does not cut the formation area of the C-curve upper bainite and the material structure is the upper bainite. According to Eq. (3.7), martensitic transformation starts (M_s temperature) at 280-286 °C (salt temperature was 290 °C) [92].

$$M_s = 512 - 453(C) - 16.9(Ni) + 15(Cr) - 9.5(Mo) + 217(C^2) - 71.5(C)(Mn) - 67.6(C)(Cr) \quad (3.7)$$

To find out the difference between the material Type I and II, the microstructure analysis on the annealed condition was carried out Fig. 3.15. First a clear difference found in the material was the grain size of the ferrite and austenite because of the use of the material casting method. Type I was produced with continuous casting and type II with ingot casting.

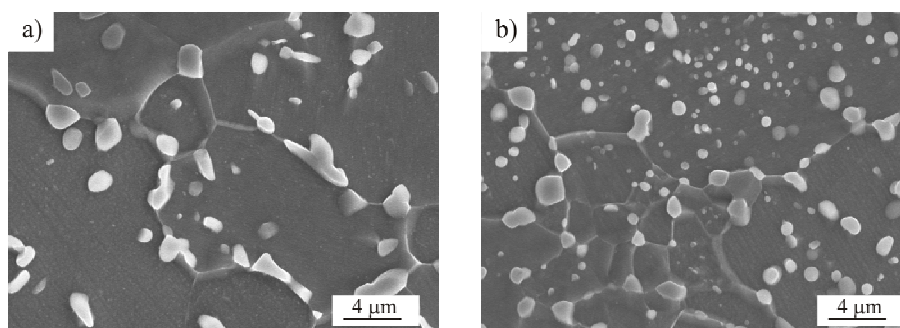


Figure 3.15 SEM pictures of steel structures: a – Type II, b – Type I

According to the theory, coarser austenite grain material should have better hardenability but practically it was the contrary [85]. It is possible that chemical elements are located differently in the structure phases. In order to determine the chemical content of ferrite and cementite, an EDS analysis was performed. The results are given in Tables 3.4. Chemical analysis showed that material type II should have better hardenability than type I because there is more or equal Mn and Cr content in the ferrite and cementite of type II.

Table 3.4 Chemical composition of ferrite and cementite of steels, wt %

Material	Ferrite			Cementite		
	Mn	Cr	Si	Mn	Cr	Si
Type I	0.4	0.2	0.3	3.6	1.4	0.0
Type II	0.5	0.2	0.3	3.8	2.2	0.1

To understand the reasons, a computer analysis method was worked out to do a detailed analysis of the material structure [Paper IV]. The structure analyses were based on the optical microscope picture in the magnification 1000X. For the structure analysis it is very important to obtain good quality microstructure because it is not easy to perform it with a soft annealed material. The grain boundaries are low angle in relative to other and therefore are not distinguished in the etching process (Fig. 3.16).

Etching was carried out with Nital (3 % HNO₃ in the ethanol and Marshall's etchant). Pre-etching of 5 to 10 s was done with Nital and 2 to 5 s etching with Marshall's etchant. For carbide etching alkaline sodium picrate (70 °C, 15-30 min with ultrasonic) was used.

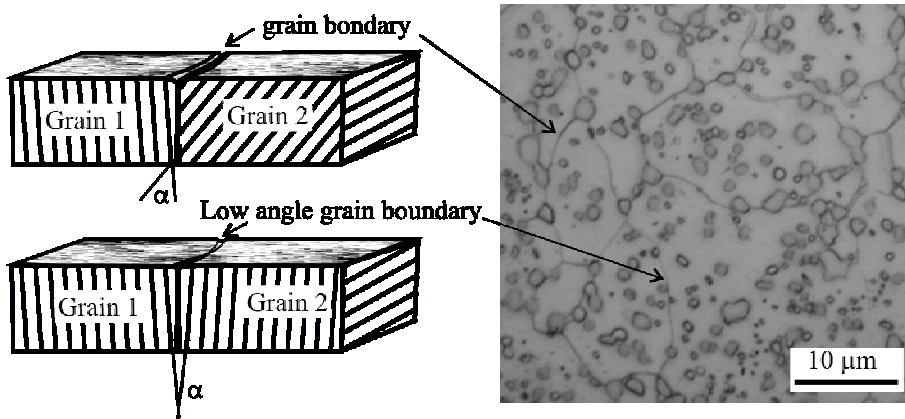


Figure 3.16 Low angle crystal structure and microstructure from optical microscope

The carbide analysis was done first to measure the carbide grain size to separate carbides and ferrite. The separation was performed according to the size. In Figs. 3.16 or 3.17 it is shown that it is not possible to separate grains otherwise.

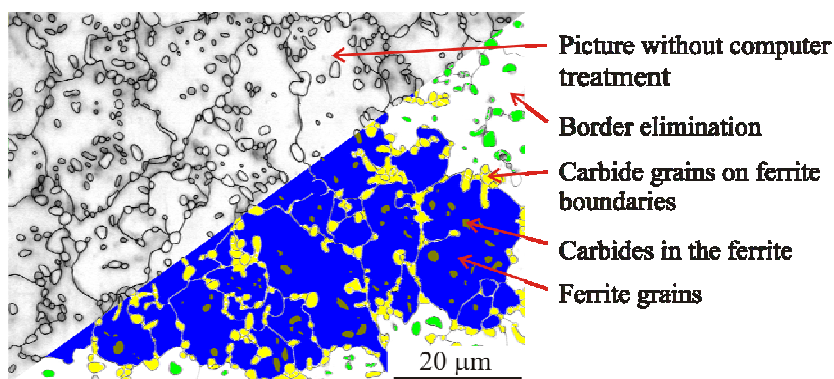


Figure 3.17 Analysed picture in the OM system

Analysis results were exported to the MS Excel because the OMS system does not allow the statistical analysis of the measured data. The distribution of the analysis results is shown in Paper IV. In carbide analysis, it is the best to obtain information based on the volume distribution because the count distribution showed no differences on the carbide size. Type II material has smaller grains by counting but they have a high volume percentage. Larger grains mean that the surface area of carbides is smaller and on the austenitization, alloying elements like Mn, Cr and C have difficulties to diffuse the matrix of austenite. Localized or larger concentration of alloying elements in the matrix of austenite leads to better recrystallization in the cooling process (C-curves move to the right).

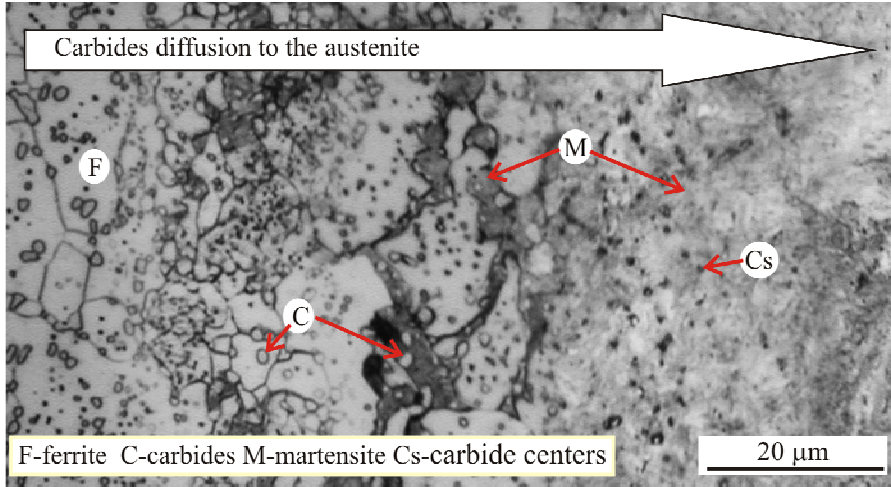


Figure 3.18 Carbide diffusion to the austenite, specimens quenched to water

The austenitization process is schematically shown in Fig. 3.18. The austenite is quenched from different austenitization temperatures (A_{e1} starting up to 100 °C over A_{e3}). A_{e1} and A_{e3} were calculated using the chemical composition of the material and Eqs. (3.8) and (3.9) [92].

$$A_{e1} = (1333 - 25Mn + 40Si + 42Cr - 26Ni - 32)5/9 \quad (3.8)$$

$$A_{e3} = (1570 - 323C - 25Mn + 80Si - 3Cr - 32Ni - 32)5/9 \quad (3.9)$$

When hardenability is better with a higher Mn and Cr content and smaller grain size of carbides (small size of carbides leads to smaller size of ferrite), then for the tool lifetime it is better to have material with low strength properties, high plasticity and equally distributed spherical carbides.

The stress R_e necessary to cause metal flow is described by the Hall-Petch relationship Eq. (3.10)

$$R_e = \sigma_{iy} + \Delta\sigma_c + \Delta\sigma_v + \Delta\sigma_0 + K_y d^{-\frac{1}{2}} \quad (3.10)$$

In Eq. (3.10) σ_{iy} is the Peierls stress, the internal friction, $\Delta\sigma_c$ is strength increase due to the inclusion atoms in the crystal lattice (alloying elements or impurities), $\Delta\sigma_v$ is the strength increase due to work hardening, $\Delta\sigma_0$ is the strength increase due to precipitation and dispersion hardening, K_y is material constant, and d is the grain diameter. The Hall-Petch law is demonstrated schematically in Fig. 3.19. To lower the forces acting on the cutting-elements of the stamp and to extend the stamp's lifetime, it is essential to lower the strength characteristics of the material. Greater plasticity characteristics and especially uniform extension provide good cutting edge quality on the final stamped part.

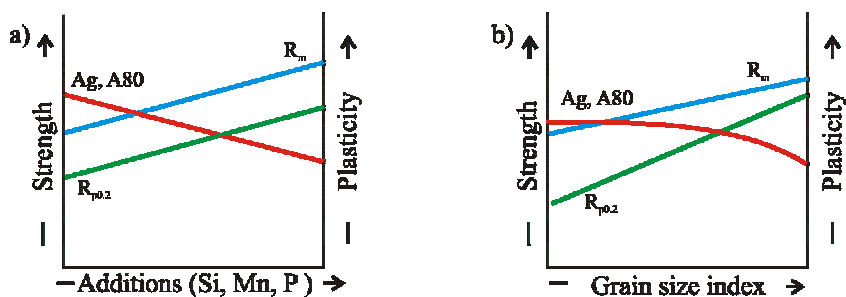


Figure 3.19 Dependence of properties determined at tensile test: a – on alloying elements and b – on G grain size

The request to produce a material with the mechanical properties shown in Table 3.5. THT with increased Mn content was considered to be an ideal material, heat-treatable in the case of larger parts and at the same time with low strength characteristics as a raw material (suitable for stamping). However, production of this type of the material is impossible (Fig. 3.19). The mechanical characteristics are closely connected to the chemical composition and microstructure, thus changing them alone is almost impossible. In THT 031 issue 5 (Table 3.5) mechanical characteristics have limits that are acceptable for material manufacturers but are too high for stamping. Therefore, it was necessary to find a new way to achieve lower mechanical strength properties.

Table 3.5 Mechanical characteristics in THT

Characteristic	THT 032 issue 3	THT 031 issue 4	THT 031 issue 5	THT 032 issue 4
R_m , N/mm ²	max 480	max 540	max 550	max 480
$R_{p0.2}$, N/mm ²	220-280	max 365	max 390	220-280
A_{80} , %	min 25	min 20	min 20	min 25
A_g , %	min 18	min 15	min 12	min 18

As it follows from Table 3.4, the Si is mostly situated in the ferrite and increases its strength (Fig. 3.19). In the case of lower Si content in the material, mechanical characteristics with the fine-grain microstructure are up to 95 % similar to the requirements of the THT 031 issue 4 (Table 3.5), but because of manufacturers' request, those requirements in the THT 031 issue 5 have not been lowered yet. While a similar effect can be witnessed with the P content, it is planned to investigate the ways of reduction of the P content and its effect on the mechanical properties. Si is an important element also in the production of an alloy (as a reducer), therefore steel melting factories are arguing that a decreased Si content can increase the non-metallic inclusion content. Based on the studies of the materials ($Si < 0.06$ %), the content of the non-metallic inclusion is similar to that of higher Si content materials.

On fineblanking, the carbide shape of the material and the distribution in the material are extremely important (Fig. 3.20). The steel microstructure shown in Fig. 3.20a is not suitable for fineblanking. This material does not correspond to THT 031 issue 5 clause 8 - Condition of Delivery and Grain: Annealed to Spheroidal Carbides > 95 %. Problems will occur with the cutting surface and tool lifetime.

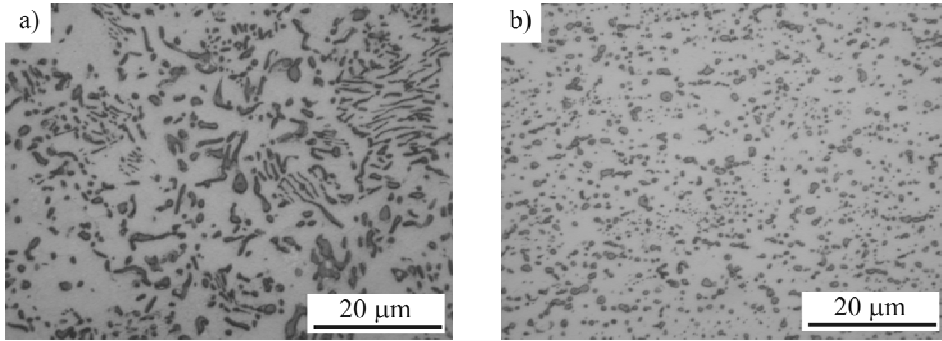


Figure 3.20 Percentage of the spheroidal carbides: a – 70 % and b – 100 %

The mechanical properties of the material are comparable (except R_m) with a good material (Table 3.6). Therefore, it was necessary to analyze steel carbide structure and find out the differences between the materials. The manufacturers give spheroidal carbides amount 100 % almost with every material batch. As it is a reason to increase the wear of a tool and the bad cutting edge on the parts, shape parameters of carbides were investigated.

$$AS_{mod_i} = \frac{length_i}{width_i} * f_i \quad (3.11)$$

$$f_i = \frac{V_i}{\sum_{i=1}^n V_i} \quad (3.12)$$

The modified shape parameter AS_{mod} Eq. (3.11) factor was worked out based on the carbide volume distribution. The frequency of f_i Eq. (3.12) emphasizes a larger grain shape. Larger grain shape can be analyzed more accurately and because of their volume, they affect material more than small ones. The results are shown in Table 3.6, where Dc is the average grain size by volume distribution and G is the average ferrite grain size index according to DIN 50601.

Based on AS_{mod} , 70 % of the material has a value of 2.6 and material with one annealing (TH I and TH II) had 2.0. These materials are not good for fineblanking. The material TW value 1.7 can be used for production, even the

mechanical properties are quite the same and plasticity can be even better (Table 3.6).

Table 3.6 Relation of structure parameters to mechanical properties

Material	AS	AS_{mod}	Dc , μm	G	$R_{p0.2}/R_m$	R_m , N/mm^2	$R_{p0.2}$, N/mm^2	$A80$, %	A_g , %
TH I	1.9	2.1	2.0	13	0.68	562	383	23	13
TH II	1.9	2.0	2.6	13	0.69	538	373	27	14
TW	1.8	1.7	3.0	13	0.68	522	355	24	12
70 % spheroidal 65G	2.5	2.6	2.3	10	0.57	598	343	22	14

In addition (beside ferrite and carbide grain size), the mechanical properties of the material affect the carbides distribution. Materials TH I and TH II were taken from the same batch. The tensile tests were too different for these samples, therefore the chemical composition and the structure were analyzed. The chemical composition was the same but the structure was different: carbide size (2.6 μm) of TH I material was smaller and carbides were on lines (segregation) (Fig. 3.21a). TH II material structure was equally distributed and had larger carbides (Fig. 3.21b). To achieve low values of strength properties, in addition to the ferrite size the chemical composition, carbide shape, size and distribution on the cross-section are essential.

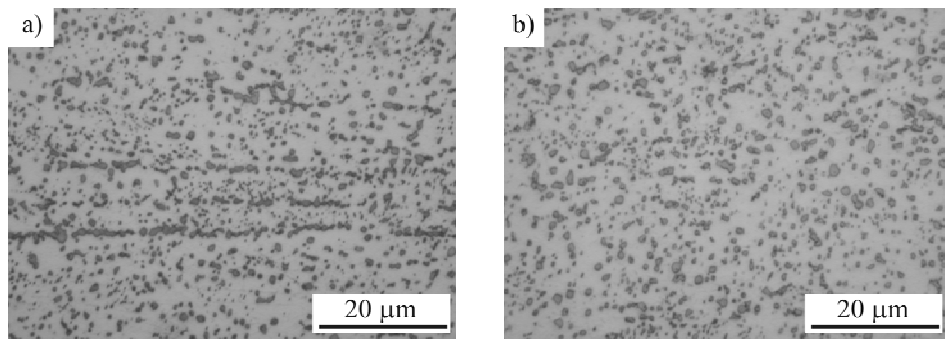


Figure 3.21 Carbide structure: a – Theis I and b – Theis II

Material with 70 % carbides has a higher percentage of Si and Mn, which increase the tensile strength; therefore this material is not affected only by structure differences like other materials in Table 3.6.

The material suitable for fineblanking should have carbide shape AS_{mod} close to 1.0 and less than 2.0. The average grain size of carbide by volume (Dc , Table 3.6) should be more than 2.0 μm and ferrite grain size according to DIN 50601 is less than 13. Preferably material should not have segregations in the structure.

3.2.2 Describing of the non-metallic inclusions in the thin sheet metal according to the DIN 50602

Non-metallic inclusions in steel can cause problems in the production as well in the use of safety belt tongues. Inclusions can affect tool lifetime, as hard particles in the structure of hardness, some inclusion is more than 1000 HV (Al_2O_3 , TiN). Those kinds of hard particles are much larger than carbides, but the frequency is many times lower.

In the steel deoxidation reactions it is better to use Al beside Si because Si increases afterwards the mechanical strength of steel and Al can ensure finer grain size together with rare earth metals [93]. Based on steel C60E non-metallic inclusion analysis, the Si content seems to increase the inclusion content in the steel and Al decreases the content of non-metallic inclusions (Figs. 3.22 and 3.23). That is one of the reasons why the Si content was decreased in the THT 031 issue 5.

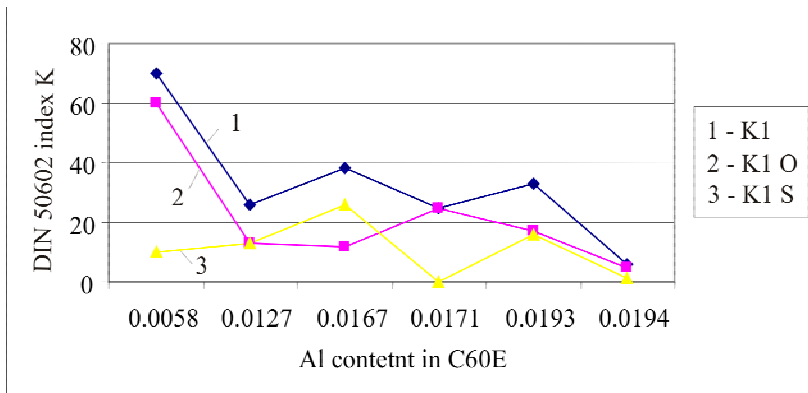


Figure 3.22 Dependence of C60E steel cleanliness on the Al content

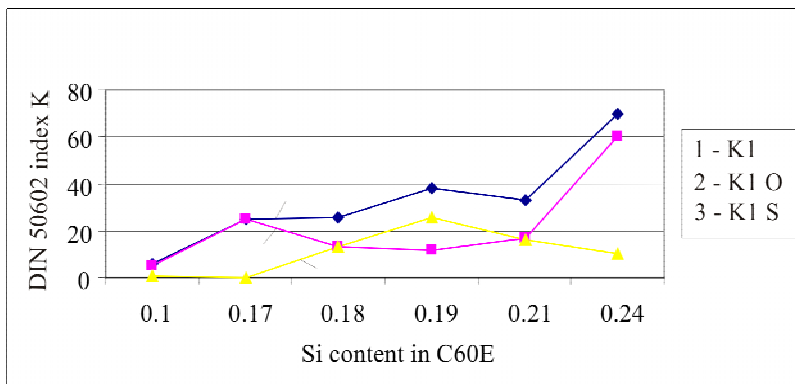


Figure 3.23 Dependence of C60E steel cleanliness on the Si content

The strict requirement of steel cleanliness were $K1 < 10$ and $M < 2$ according to the DIN 50602, to be controlled to prove that the requirement is well grounded. With computer analysis it can be easier to make several measurements and obtain the inclusion content by the K1 method. The main problem of computer analysis is the recognition of non-metallic inclusions. Therefore, different preparation techniques are used to obtain the “clear” picture and the OMS system is used to measure the sulphides and oxides in the steel. Finally, computer analysis methods based on DIN 50602 M and K to describe the non-metallic inclusions were worked out (separately sulphides and oxides) in. To control the system, the reference test was performed with Risse+Wilke Kaltband GmbH&Co (Table 3.7).

Table 3.7 Reference test with Risse+Wilke Kaltband GmbH&Co

		Steel 60 G				K1 total
Risse+Wilke	Sulphides	66.4	115	98	119.8	
	Oxides	2.4	9.72	3.2	3.24	
	Sum	68.8	124.7	101.2	123.04	
TUT	Sulphides	45	58.2	68.9	85.2	
	Oxides	2.6	5.3	3.8	1.3	
	Sum	48	63	73	86	

In the materials analyzed at TUT, the amount of non-metallic inclusions was higher and the average is $K1 = 30...40$. By the certificate, $K1 = 3...10$. Steel producers analyze the results from the casting products using the ultrasonic and metallographic methods. The amount of inclusion remains unchanged during rolling but the shape will change. The analysis of TUT inclusions in thin sheet metal showed that these are very thin and long. All the methods focus on the analysis of the content of non-metallic inclusions that are not designed for thin sheet metals.

The problems occurring in the course of production connected to non-metallic inclusions have not been observed. But hard inclusions can cause tool scratches randomly and it can be the reason for fatigue. This process can not be controlled because of too many variables which should first be eliminated. The material with the non-metallic inclusion content $K1$ about 100-200 is problematic in the production, at the same there is no significant risk with the material non-metallic inclusions under $K1 < 60$ and $M < 3$. To guarantee the conditions, the real non-metallic inclusion content on the material must be established.

From this part the following conclusions may be drawn:

- To analyze the C60E structure (annealed to spherical carbides) it is necessary to use count and volume size distribution. The structure differences can appear on the count distribution (in this case ferrite size) or volume size distribution (carbide size).

- The main difference is that type I has many small ferrite grains by count distribution and smaller carbides by volume distribution. The material type I has higher strength properties in annealed condition and better harden-ability than material type II.
- The material is suitable for fineblanking should have carbide shape AS_{mod} close to 1.0 and less than 2.0. Preferably material should not have segregations in the structure
- Decrease R_m 550 N/mm² => 540 N/mm² to and use the index $R_{p0,2}/R_m = 0.6$ max to increases the stamping tools lifetime.
- Carbide average grain size by volume should be between 2.0 – 3.8 μm and ferrite grain size index (DIN 50601) between 10 – 13
- To assure the hardenability Mn content should be 0.6 – 0.7 and carbide grains less than 3.8 μm
- Higher Al content reduces the non-metallic inclusion content in the C60E and Si gives contrary result
- The calculation of K and M of DIN 50602 method is quite easy if there is good information from earlier steps, metallographic preparation and recognition of different non-metallic inclusions.
- DIN 50602 has some aspects, which are not described mathematically and are done by ISO 4967, difference between oxide and sulphide with aspect ratio and separating or closing long inclusions.
- Reference material and test are necessary to carry out to control the measuring method.
- Changing the chemical composition P = 0.015 % => P = 0.01 % and S = 0.008 % => S = 0.005 %. Decreases embrittlement and ferrite strength.
- Decreasing the quality level of non-metallic inclusions K1 < 10 to K1 < 30 (if it influences to price) or use K4 method. Currently there are lower quality materials in the production process with no problems. Experience has shown that the problems in the production starts from K1 > 100 – 200.
- To describe the non-metallic inclusions M method should be used together K method, target M2-M3 to avoid rare large non-metallic inclusions, which may cause sudden breakdown of detail or stamping tool.

CONCLUSIONS

1. Special metallographic preparation methods were developed to distinguish the structure phases for computer analysis. Different grain size measuring principles and distributions were used to study the microstructure.
2. The methods adequately describing the WC-Co powder and granules size, shape, microstructure and composition were specified. Micropowders should be analysed with a laser particle analyser and controlled by image analysis (using volume distribution) and shape parameter aspect ratio should be measured. Granules structure should be analysed by volume distribution from cross-section using SEM pictures.
3. A method to describe the bimodal WC-Co abrasive resistant coating microstructure was developed. The WC grains spherical diameter from SEM images should be measured and volume distribution calculated based on it. The modes should be characterized by size and volume amount of larger particles.
4. Microstructure analyses of coatings enable us to show that particular WC particle volume distribution (uniform distribution of small-size hard particles (about 1 μm) and a certain amount (5 to 10 % by volume) of larger hard particles (2 to 3 μm)) is one of the main reasons of good abrasive wear resistance. High porosity of a coating (about 2 to 3 %) can reduce its wear resistance.
5. The steel C60E modifications (chemical composition and microstructure) with economically reasonable price were worked out, where production has higher quality. The steel should have carbide shape AS_{mod} close to 1.0 and less than 2.0. Preferably material should not have segregations in the structure. Carbide average grain size by volume should be smaller than 3.8 μm and ferrite grain size G between 10-13.
6. The factors that lead to the hydrogen embrittlement are connected with poor hardenability (upper bainite) or with high hardness of material (stresses in material).

Future plans

1. To produce mechanically alloyed WC-Co granules with different parameters and grain sizes to develop a new method for HVOF granules production.
2. To test different grades of steel and high strength micro alloyed steels for safety belt tongues production.
3. To specify the parameters which affect the tool lifetime in conventional and fine blanking.
4. To develop fully automatic structure analysis methods to describe the steel non-metallic inclusions and microstructure.

KOKKUVÕTE

Sepad on muistsetel aegadel teinud väga häid nugasid ja mõõku, olenemata teadmistest mikrostruktuurist ja materjalidest. Seda olen õppinud nende sepieste mikrostruktuure uurides. Tänapäeval on materjalide uuringuteks head vahendid, kuid sellele vaatamata on paljusid seoseid materjalides raske seletada. Kohati käitume sarnaselt iidsete aegade seppadega – teeme detaili valmis, katsetame seda ja kui see töötab, üritame ohvreid tuua samadele jumalatele.

Antud töös on uuritud kahte sorti materjale: WC-Co pinne ja madallegeeritud teras C60E. WC-Co materjali on kasutatud abrasiivkulumiskindla pinde valmistamiseks kiirleekpihustuse seadmega. Pihustuse pulber on valmistatud mehaanilise aktiveerimise teel nanomeetrilisest pulbrist. Pinde mikrostruktuur koosneb submikromeetrilisest/nanomeetrilisest ja mikromeetrilistest WC ja $W_xCo_yC_z$ osakestest.

Madallegeeritud terast C60E kasutatakse turvavöö keelte valmistamiseks. Turvavöö keeled valmistatakse silelöikestantsimisel lehtmaterjali rullidest. Tugevusomaduste saavutamiseks kasutatakse keeltele isothermkarastust alabeiniitstruktuurile. Välimuse saab turvavöö keel Ni-Cr galvaniseerimisel, mida on antud töös käsitletud kui atomaarse vesiniku põhjustajat ja sellest tuleneva vesinikhapruse tekitajat.

Töö üldine eesmärk on mikrostruktuurianalüüsi meetodite väljaarendamine, baseerudes uuritavatele eesmärkidele ja kasutades peamiselt arvutianalüüsi. Uuritavateks eesmärkideks on materjali erinevate omaduste (mehaanilised ja tehnoloogilised omadused) ja mikrostruktuuri vaheliste seoste selgitamine.

Kirjanduse analüüsist tulenevalt ei ole WC-Co mikrostruktuuri uurimise meetodid ja esitatud arv-väärtused määratletud täpselt, kuid samas sõltub tulemus oluliselt valitud meetoditest. Mehaanilisel aktiveerimisel valmistatud komposiitpulbri granulomeetria analüüsil on nüansid erikujuga pulbrite analüüsil. Bimodaalse mikrostruktuuri kirjeldamiseks puuduvad konkreetsete numbrilised väljundid mõlema moodi kirjeldamisel.

Terase C60E aktuaalsus on seotud terase hinna tõusuga maailmaturul, mistõttu tuli kasutusele võtta teistsuguse keemilise koostisega, madalama Cr sisaldusega teras. Kirjandusest tulenevalt võib öelda, et puuduvad uuringud mikrostruktuuri mõjust paralleelselt silelöikestantsimisele ja isothermkarastamisele. Terasel mikrostruktuuri uuringute käigus selgus, et standardsed meetodid ei too välja kõiki mikrostruktuuri nüansse.

Dokoritöö eesmärgid võib jagada materjalidest ja teema aktuaalsusest tulenevalt alaeesmärkideks:

1. WC-Co komposiitpulbri osakese suuruse, kuju ja mikrostruktuuri uuringu meetodite nüansside väljaselgitamine. HVOF pinde mikrostruktuuri analüüsi meetodite edasiarendamine ja mikrostruktuuri seos pinde abrasiivkulumiskindlusega.
2. Terasel C60E aktuaalsus on seotud vajadusega defineerida materjali parameetrid nii, et selle töödeldavus oleks optimaalne ja toodang kvaliteetne.

Terase C60E materjali mikrostruktuuri uuringute meetodite edasiarendamine (lõõmutatud struktuurid).

3. Materjali mikrostruktuuri ja keemilise koostise mõju hindamine silelõikestantsimisel ja isothermkarastamisel ning vesinikhaprust põhjustavate tegurite piiritlemine.

Doktoritöö tegemisel on rakendatud erinevaid materjali uurimise meetodeid. Granulomeetrilise koostise määramisel: sõelanalüüs, laseranalüüs, kujutise analüüs, eripind ja XRD. Keemilise koostise määramisel: aatomemissioonspektroskoopia sädelahendusel, elementaaranalüüs, mass-spektroskoopia, EDS, WDS ja metallograafilised meetodid. Metallograafilisel analüüsil kasutati optilist mikroskoopi, SEM, EDS, XRD, mikrokõvadust (Vickers), mikrostruktuuri uurimise programme Image Pro 3.1 ja Omnimet Image Analysis System 4.1, standardmeetodeid DIN 50602, ISO 643, ASTM E112, DIN 50601, ISO 84967 EN 1245, SEP 1520 ja ISO 3887. Mehaaniliste omaduste uurimisel rakendati kõvaduse mõõtmisel *HRC* ja *HV*, tõmbeteimil vastavalt EN 100021-1 $R_{p0,2}$, R_m , A_g ja A_{80} . Eriotarbeliselt keelte keelte paindekatsse, tõmbekatsse ja termotöödeldud tõmbekatssekehade katsetamine terase läbikarastuvuse määramiseks.

Töö tulemusel loodi meetodid materjalide kirjeldamiseks arvutianalüüsi kasutades. Mikrostruktuuri prepareerimiseks arendati spetsiifilised meetodid, lähtudes arvutianalüüsi vajadusest. Arvutianalüüsi tulemuste esitamiseks leiti sobivad väljundid, mis on mikrostruktuuri kirjeldamise numbriline väljund. Töö peamised järeldused:

1. Töötati välja spetsiaalsed metallograafilise prepareerimise meetodid mikrostruktuuri erinevate faaside eristamiseks arvutianalüüsil. Kasutati erinevaid tera suuruse mõõtmise meetodeid ja jaotisi (sagedus, pindala, ruumala ja kaalu jaotis) mikrostruktuuri kirjeldamiseks.
2. Täpsustati meetodid, millega adekvaatselt kirjeldada mikropulbreid ja -graanuleid. Mikropulbrite suuruse analüüsiks on sobivam laseranalüüs ja tulemuse kontrolliks osakeste suuruse kujutiseanalüüs ristlihvalt. Kujuparameetritest on sobivaim elliptilisus *AS*. Graanulite mikrostruktuuri analüüsiks kasutatakse SEM mikrostruktuuri pilte ja sama meetodikat pinde mikrostruktuuri analüüsiga.
3. Bimodaalse abrasiivkulumiskindla WC-Co pinde mikrostruktuuri kirjeldamiseks arendati uus meetod. WC osakeste sfäärilise diameetri alusel arvutatakse nende ruumala jaotis ja tuuakse välja ruumala jaotise statistilised näitajad. Bimodaalse mikrostruktuuri iseloomustamiseks tuuakse välja mõlema moodi keskväärtus ja protsent ruumala järgi.
4. Bimodaalse WC-Co pinde abrasiivkulumiskindluse tagab ruumala jaotuse järgi moodiga 0.5-2 μm ja 5-10 % suuremaid 3-4 μm moodiga WC terad ning väike poorsus alla 2-3 %.
5. AS Norma on saanud töö tulemusena materjali THT, mille järgne materjal on sobilik kõikidele tootmise operatsioonidele ja toodang on kvaliteetsem majanduslikult ökonoomsemalt.

6. Teras peaks koosnema Mn 0.6...0.65 %, Si alla 0.06 %; mikrostruktuuris peaks olema karbiidide kuju AS_{mod} järgi 1.0...2.0. Karbiidide osas ei tohi olla segretatsioonid, karbiidide tera suurus peab olema alla 3.8 μm ja ferriidi tera suuruse indeks $G = 10...13$ (DIN 50601).
7. Vesinikhaprus on tingitud ebapiisavast läbikarastuvusest ja ülabeiniitstruktuurist ja/või liiga suurest kõvadusest (suurematest sisepingetest).

Soovitused WC-Co materjali mikrostruktuuri uuringuteks ja abrasiivkulumiskindluse ning mikrostruktuurivaheliste seoste leidmiseks:

- Kasutada WC-Co materjali mikrostruktuuri uurimisel ruumala jaotust, mis toob välja erinevused ja ühtib pulbri analüüsi põhimõtetega ning näitab tegelikku tera kasvu erinevates operatsioonides.
- Bimodaalse abrasiivkulumiskindla pinde uurimisel tuleb kirjeldada mõlemad moodid ruumala jaotuses nii suuruselt kui ka osakaalult.
- Pulbritel tuleb granulomeetrilise koostise määramisel kontrollida lisaks pulbri kuju, et veenduda saadud tulemuse õigsuses.
- Komposiitpulbri mikrostruktuuri uurimisel tuleb rakendada sarnaseid põhimõtteid pinde mikrostruktuuri uurimisega ja avatud poorsuse määramisel saab kasutada graanuli eripinna määramist.

Soovitused terase C60E kasutamiseks silelõikestantsimisel ja isothermkarastamisel:

- Termotöödeldavuse hindamiseks tuleb uurida materjali keemilist koostist ja mikrostruktuuri. Silelõikestantsitavuse määramiseks tuleb analüüsida materjali mehaanilisi omadusi ja karbiidide kuju.
- Muuta keemilist koostist $P = 0.015\%$ \Rightarrow $P = 0.01\%$, $Si = 0.23\%$ \Rightarrow $Si = 0.06\%$. Vähendab haprust ja ferriidi tugevust, vähenevad tugevusnäitajad.
- Vähendada nõudmisi mittemetalsetele lisanditele $K1 < 10 \Rightarrow K1 < 30$ (kui alandab terase hinda ja laiendab tarnijate ringi) või minna üle K4 meetodile.
- THT-s muuta nõuded austeniidi tera suuruse indeksile ferriidi tera suuruse indeksiks $G > 10$.

REFERENCES

1. Metals Handbook, second edition, Volume 9, Metallography and microstructures. ASM International Materials Park, Ohio, USA, 1998.
2. Particular Guide to Image Analysis. ASM International, 2000.
3. Jenkins, R., Snyder, L.R. Introduction to X-Ray Powder Diffractometry. John Wiley & Sons, Inc., 1996.
4. Metals Handbook, second edition, Volume 3, Alloy and Phase Diagrams. ASM International Materials Park, Ohio, USA, 1998.
5. Metals Handbook, second edition, Volume 10, Materials Characterization. ASM International Materials Park, Ohio, USA, 1998.
6. <http://www.buehler.com> (10.02.07)
7. <http://www.struers.com> (10.02.07)
8. Merle, P., Metallographic Preparation of Metal Matrix Composites. MMC-Assess Consortium, August 2000.
9. Johnson, C., Metallography Principles and Procedures. Leco digitally printed, 2006.
10. Vander Voort, G. F., Color Metallography. – *Microscopy and Microanalysis*. 2004, 10(2), pp. 70–71.
11. Vander Voort, G. F., Metallography: Principles and Practice, ASM International, Materials Park, Ohio, 1999, pp. 223–224.
12. Vander Voort, G. F., Manilova, E. P., Michael, J. R., Lucas, G. M. Study of Selective Etching of Carbides in Steel. Published online by Cambridge University Press, 01 August 2004.
13. Vander Voort, G. F., Color Metallography. *Microscopy Today*, Microscopy Society of America, November 2005, pp. 22–27.
14. Buehler, Sum-Met. The Science Behind Materials Preparation. Buehler Ltd., USA, 2004.
15. Vander Voort, G. F., Manilova, E. P., Michael, J. R., Lucas, G. M. Study of Selective Etching of Carbides in Steel. – *Microscopy and Microanalysis*. 2004, 10(2), pp. 76–77.
16. Šuška, J., Mišicko, R. P., Fujda, M., Kvackaj, T., Molnarova, M. Etching Technique and Microstructure Components Identification in Trip Steels. – *Acta Metallurgica Slovaca*. 2007, (13), pp. 113–117.
17. Mikli, V., Kulu, P., Käerdi, H. Application of Image Analysis Methods to Characterize the Impact-Milled WC-Co Powder Particles. – *Image Analysis & Stereology*. 2001, (20), pp. 199–204.
18. Mikli, V. Electron Microscopy and Image Analysis Study of Powdered Hardmetal Materials and Optoelectronic Thin Films, PhD Thesis. TTÜ Press, 2003.
19. Kulu, P., Mikli, V., Käerdi, H., Besterci, M. Characterization of Disintegrator Milled Hardmetal Powder. – *Journal of Powder Metallurgy Progress*. 2003, 3(1), pp. 39–48.

20. Mikli, V., Kulu, P., Käerdi, H., Bestercei, M. Angularity of the Disintegrated Ground Hardmetal Powder Particles. – *Materials Science (Medžiagotyra)*. 2002, (4), pp. 430–433.
21. Kohutek, I., Bestercei, M., Kulu, P., Mikli, V., Velgosova, O. WC-Co Powders Particles Morphological Characteristics. *In: Proceeding of the International Conference Deformation and Fracture in Structural PM Materials DF PM2002*. 2002, (2), pp. 230–235.
22. Mikli, V., Käerdi, H., Kulu, P., Bestercei, M. Characterization of Powder Particle Morphology. – *Proceedings of the Estonian Academy of Sciences. Engineering*. 2001, (1), pp. 22–34.
23. Kohutek, H., Kaerdi, H., Kulu, P., Sylleiova, K., Velgosova, O., Mikli, V., Bestercei, I. Particles Morphology Description by Image Analysis. – *Acta Metallurgica Slovaca*. 2000, pp. 256–260.
24. Mikli, V., Kulu, P., Käerdi, H. WC-Co Hardmetal Powders for Formation of Wear Resistant Coatings. *In: Proceedings of the 2nd International Conference. 27-29 April 2000, Tallinn, Estonia. Tallinn, 2000*, pp. 201–204.
25. Kulu, P., Zimakov, S. Wear Resistance of Thermal Sprayed Coatings on the Base of Recycled Hardmetal. – *Surface and Coatings Technology*. 2000, (130), pp. 46–51.
26. Kulu, P., Pihl, T., Zimakov, S. Wear Resistance of Thermal Sprayed Coatings. *In: Proceeding of International Conference Baltrib'99. Kaunas, 1999*, pp. 311–318.
27. Mikli, V., Kulu, P., Tarbe, R., Peetsalu, P., Zimakov, S. Recycled Hardmetal Based Powders for Thermal Spray. – *Proceedings of the Estonian Academy of Sciences. Engineering*. 2004, 10(4), pp. 315–325.
28. Kulu, P., Mikli, V., Käerdi, H., Bestercei, M. Characterization of Disintegrator Milled Hardmetal Powder. – *Journal of Powder Metallurgy Progress*. 2003, 3(1), pp. 39–48.
29. Zimakov, S., Pihl, T., Kulu, P., Antonov, M., Mikli, V. Applications of Recycled Hardmetal Powder. – *Proceedings of the Estonian Academy of Sciences. Engineering*. 2003, 9(4), pp. 304–316.
30. Zimakov, S., Peetsalu, P., Pirso, J., Kulu, P., Mikli, V. Thermal spray coatings from WC-Co powders produced by mechanically activated synthesis. *In: Thermal Spray 2006: Building on 100 Years of Success + Proceedings of International Thermal Spray Conference (ITSC) & Exposition, 15-18 May 2006, Seattle, USA. [CD-ROM]: International Thermal Spray Conference (ITSC) & Exposition, 15-18 May 2006, Seattle, USA. Marple, B. R., Hyland, M. M., Lau, Y.-C., Lima, R. S., Voyer, J. ASM International, 2006*.
31. Zhua, Y. C., Dingb, C. X., Yukimurac, K., Xiao, T. D., Strutt, P. R. Deposition and Characterization of Nanostructured WC–Co Coating. – *Ceramics International*. 2001, (27), pp. 669–674.
32. Jarosinski, W. J., Gruninger, M. F., Londry, C. H. Characterization of Tungsten Carbide Cobalt Powders and HVOF Coatings. *In: Proceedings*

- of the 1993 National Thermal Spray Conference, Anaheim, CA. 1993, pp. 153–157.
33. Schwetzke, R., Kreye, H. Microstructure and Properties of Tungsten Carbide Coatings Sprayed With Various HVOF Spray Systems. *In: Proceedings of the 15th International Thermal Spray Conference, 25–29 May 1998, Nice, France. 1998, pp. 187–192.*
 34. Nerz, J., Kushner, B., Rotolico, A. Microstructural Evaluation of Tungsten Carbide-Cobalt Coatings. – *Journal of Thermal Spray Technology. 1992, 1(2), pp. 147–152.*
 35. Schwetzke, R., Kreye, H. Microstructure and Properties of Tungsten Carbide Coatings Sprayed With Various HVOF Spray Systems. *In: Coddet, C. (Ed.) Thermal Spray: Meeting the Challenges of the 21st Century Vol. 1, ASM International, Metals Park, OH. 1998, pp. 187–192.*
 36. Rangswamy, S., Herman, H. Metallurgical Characterization of Plasma Sprayed WC–Co Coating. *In: Proceedings of 11th International Thermal Spraying Conference, 8–12 September 1986, Montreal, Canada. WIC, Canada, 1986, pp. 101–110.*
 37. Upadhyaya, G. S. Materials Science of Cemented Carbides – an Overview. – *Materials and Design. 2001, (22), pp. 483–489.*
 38. Schultrich, B., Berger, L. M., Menker, J., Oswald, A. Influence of Carbide Powder Composition on Decarburization During Air Plasma Spraying. *In: Eschnauer, H. (Ed.). Proceedings of 2nd Plasma-Technik Symposium, Lucerne, Switzerland. 1991, (2), pp. 363–371.*
 39. Korpiola, K. High Temperature Oxidation of Metal, Alloy and Cermet Powders in HVOF Spraying Process, PhD Thesis. Helsinki University of Technology Publications in Materials Science and Metallurgy. TKK-MK-160. Espoo, 2004.
 40. Khan, M. S. A., Clyne, T. W. Microstructure and Abrasion Resistance of Plasma Sprayed Cermet Coatings. *In: Proceedings of the 9th National Thermal Spray Conference, Thermal Spray: Practical Solutions for Engineering Problems, 7–11 October 1995 Cincinnati, OH. 1995, pp. 113–121.*
 41. Verdon, C., Karimi, A., Martin, J. L. Microstructural and Analytical Study of Thermally Sprayed WC–Co Coatings in Connection With Their Wear Resistance, *Material Science Engineering. 1997 (A 234–236), pp. 731–734.*
 42. Celika, E., Culhaa, O., Uyulgana, B., Ak Azema, N. F., Ozdemira, I., Turk, A. Assessment of Microstructural and Mechanical Properties of HVOF Sprayed WC-based Cermet Coatings for a Roller Cylinder. – *Surface & Coatings Technology. 2006, (200), pp. 4320–4328.*
 43. Liao, H., Normand, B., Coddet, C. Influence of Coating Microstructure on the Abrasive Wear Resistance of WC-Co Cermet Coatings. – *Surface and Coatings Technology. 2000, (124), pp. 235–242.*

44. Yang, Q., Senda, T., Ohmorib, A. Effect of Carbide Grain Size on Microstructure and Sliding Wear Behavior of HVOF-sprayed WC–12 % Co Coatings. – *Wear*. 2003, (254), pp. 23–34.
45. Usmani, S., Sampath, S., Huock, D.L., Lee, D. Effect of Carbide Grain Size on the Sliding and Abrasive Wear Behaviour of Thermally Sprayed WC-Co Coatings. – *Tribology Transactions*. 1997, (40), pp. 470–478.
46. Yang, Q., Senda, T., Ohmorib, A. Effect of Carbide Grain Size on Microstructure and Sliding Wear Behavior of HVOF-sprayed WC–12 % Co Coatings. – *Wear*. 2003, (254), pp. 23–34.
47. Baik, K. H., Kimb, J. H., Seong, B. G. Improvements in Hardness and Wear Resistance of Thermally Sprayed WC-Co Nanocomposite Coatings. – *Materials Science and Engineering*. 2007, (A 449–451), pp. 846–849.
48. Stewart, D. A., Shipway, P. H., Mc Cartney, D. G. Microstructural Evolution in Thermally Sprayed WC-Co Coatings: Comparison Between Nanocomposite and Conventional Starting Powders. – *Acta mater*. 2000, (48), pp. 1593–1604.
49. DIN 50602 1985 Microscopic Examination of Special Steels Using Standard Diagrams to Assess the Content of Non-Metallic Inclusions.
50. EVS-ISO 84967:2005 Steel-Determination of Content of Non-Metallic Inclusions – Micrographic Method Using Standard Diagrams.
51. SEP 1520 1978-03 Microscopic Examination of Carbide Structure in Steels by Means of Diagram Series.
52. DIN 50601 1985 Determination of the Ferritic or Sustenitic Grain Size of Steel and Ferrous Materials.
53. EVS-EN ISO 643:2003 Steels – Micrographic Determination of the Apparent Grain Size.
54. ASTM E 112 1996 Standard Test Methods for Determining Average Grain Size.
55. EVS-EN ISO 3887:2004 Steels – Determination of Depth of Decarburization.
56. ASTM E1245-03 Standard Practice for Determining the Inclusion or Second-Phase Constituent Content of Metals by Automatic Image Analysis
57. E1245-03 Standard Practice for Determining the Inclusion or Second-Phase Constituent Content of Metals by Automatic Image Analysis.
58. Sudhakar, K. V. Failure Analysis of an Automobile Valve Spring. – *Engineering Failure Analysis*. 2001, (8), pp. 513–520.
59. Riedel, U. T., Bleck, W., Morgan, J. E., Guild, F. J., McMahon, C. A. Finite Element Modelling of the Effect of Non-Metallic Inclusions in Metal Forming Processes. – *Computational Materials Science*. 1999, (16), pp. 32–38.
60. Chen, Z. H., Tang, C. Y., Lee, T. C., Chan, L. C. Numerical Simulation of Fine-Blanking Process Using a Mixed Finite Element Method. – *International Journal of Mechanical Sciences*. 2002, (44), pp. 1309–1333.

61. Mediavilla, J., Peerlings, R. H. J., Geers, M.G. D. An Integrated Continuous-Discontinuous Approach Towards Damage Engineering in Sheet Metal Forming Processes. – *Engineering Fracture Mechanics*. 2006, (73), pp. 895–916.
62. Chen, Z. H., Tang, C. Y., Lee, T. C. An Investigation of Tearing Failure in Fine-Blanking Process Using Coupled Thermo-Mechanical Method. – *International Journal of Machine Tools & Manufacture*. 2004, (44), pp. 155–165.
63. Eriksson, R., Jönsson, P., Gustafsson, A. Determination of Inclusion Characteristics in Low Carbon Steel During Up-Hill Teeming. – *Scandinavian Journal of Metallurgy*. 2004, (33), pp. 160–171.
64. Metals Handbook, second edition, Volume 1, Properties and Selection: Irons, Steels, and High-Performance Alloys. ASM International Materials Park, Ohio, USA, 1993.
65. <http://www.videotest.ru/> (10.02.07)
66. <http://www.clemex.com/> (10.02.07)
67. <http://www.cns21.com/> (10.02.07)
68. <http://www.spectro-systems.ru/> (10.02.07)
69. <http://www.microscopy.olympus.eu/> (10.02.07)
70. <http://rus-art.com/ww/siams.com/> (10.02.07)
71. <http://www.nexsys.ru/> (10.02.07)
72. <http://www.jomesa.com/> (10.02.07)
73. <http://www.olsysia.co.kr/> (10.02.07)
74. Cabalin, L. M., Mateo, M. P., Laserna, J. J. Large Area Mapping of Non-Metallic Inclusions in Stainless Steel by an Automated System Based on Laser Ablation. – *Spectrochimica Acta*. 2004, Part B (59), pp. 567–575.
75. Müller, G., Stahnke, F., Bleiner, D. Fast Steel-Cleaness Characterization by Means of Laser Assisted Plasma Spectrometric Methods. – *Talanta*. 2006, (70), pp. 991–995.
76. Aktinson, H. V., Shi, G. Characterization of Inclusions in Clean Steels: A Review Including the Statistics of Extremes Methods. – *Progress in Materials Science*. 2003, (48), pp. 457–520.
77. Gammer, K., Rosner, M., Poeckl, G., Hutter, H. AES and SIMS Analysis of Non-Metallic Inclusions in a Low-Carbon Chromium-Steel. – *Analytical and Bioanalytical Chemistry*. 2003, (376), pp. 255–259.
78. <http://www.oxinst.com/wps/wcm/connect/Oxford+Instruments/Products/Microanalysis/INCASteel/INCASteel> (10.02.07)
79. Cold Forming and Fineblanking – A Handbook on Cold Processing, Material Properties, Part Design. Edelstahlwerke Buderus AG, Feintool AG Lyss, Hoech Hohenlimburg GmbH, Kaltwalzerk Brockhaus GmbH. Switzerland, 1997.
80. Thipprakmas, S., Jin, M., Murakawa, M. An Investigation of Material Flow Analysis in Fineblanking Process. – *Journal of Materials Processing Technology*. 2007, (192–193), pp. 237–242.

81. Zheng, P. F., Chan, L. C., Lee, T. C. Numerical Analysis of the Sheet Metal Extrusion Process. – *Finite Elements in Analysis and Design*. 2005, (42), pp.189–207.
82. Xiao-Long, X., Zheng, Z., Song, Y., Sheng-Guang, G., Jun, C., Ming-Hui, L. Mechanism of Localized Severe Plastic Deformation and Damage Fracture in Fine-Blanking Using Mixed Displacement and Pressure FEM. – *Transactions of Nonferrous Metals Society of China*. 2006, (16), pp. 1021–1028.
83. Klocke, F., Sweeney, K., Raedt, H.-W. Improved Tool Design for Fine Blanking Through the Application of Numerical Modeling Techniques. – *Journal of Materials Processing Technology*. 2001, (115), pp. 70–75.
84. Chen, Z. H., Chan, L. C., Lee, T. C., Tang, C. Y. An Investigation on the Formation and Propagation of Shear Band in Fine-Blanking Process. – *Journal of Materials Processing Technology*. 2003, (138), pp. 610–614.
85. Nagu, G. A., Amarnath, Namboodhiri, T. K. G. Effect of Heat Treatments on the Hydrogen Embrittlement Susceptibility of API X-65 Grade Line-Pipe Steel. – *Indian Academy of Sciences Bulletin of Materials Science*. June 2003, 26(4), pp. 435–439.
86. Metals Handbook, Volume 4, Heat Treating. ASM International Materials Park, Ohio, USA, 1991.
87. Bhadeshia, H. K. D. H. Bainite in Steels Transformations, Microstructure and Properties. IOM Communications Ltd. London, England, 2001.
88. Garcia-Mateo, C., Bhadeshia, H. K. D. H. Nucleation Theory for High-Carbon Bainite. – *Materials Science and Engineering: A*. 2004(A378), pp. 289–292.
89. Offerman, S. E., van Dijk, N. H., Sietsma, J., Grigull, S., Lauridsen, E. M., Margulies, L., Poulsen, H. F., Rekveldt, M. Th., van der Zwaag, S. Grain Nucleation and Growth During Phase Transformations. – *Science*. 1 November 2002, (298), pp. 1003–1005.
90. Garcia-Mateo, C., Caballero, F. G., Bhadeshia, H. K. D. H. Development of Hard Bainite. – *ISIJ International*. 2003, 43(8), pp. 1238–1243.
91. Caballero, F. G., Bhadeshia, H. K. D. H., Mawella, K. J. A., Jones, D. G., Brown, P. Very Strong Low Temperature Bainite. – *Materials Science and Technology*. March 2002, (18), pp. 279.
92. <http://www.keytosteel.com> (02.10.2007)
93. Metals Handbook Desk Edition, ASM International Materials Park, Ohio, USA, 1998.
94. Mechanical Engineers' Handbook – Materials and Mechanical Design, 3rd Edition. John Wiley & Sons, Inc., Hoboken, New Jersey, 2006.
95. Matsuzaki, A., Bhadeshia, H. K. D. H. Effect of Austenite Grain Size and Bainite Morphology on Overall Kinetics of Bainite Transformation in Steels. – *Materials Science and Technology*. May 1999, (15), pp.518–522.
96. Durand-Charre, M. Microstructure of Steels and Cast Irons. Originally published in French as La microstructure des aciers et des fontes. Gen&se et interpretation, Ed. SIRPE. Paris, 2003.

97. Final Project Report: An Assessment of Magnetization Effects on Hydrogen Cracking for Thick Walled Pipelines. Center for welding joining & coatings research department of metallurgical & materials engineering. USA, 2005.
98. Oriani, R. A., Hirth, J. P., Smialowski, M. Hydrogen Degradation of Ferrous Alloys. Noyes Publications, Mill Road, Park Ridge, New Jersey, USA, 1985.
99. Stevens, M.F. Analysis of Trapping Effects on Hydrogen Embrittlement of a HSLA Steel. *In: Proceedings of the Third International Conference on Effect of Hydrogen on Behavior of Materials*, the Metallurgy Society of AIME, Wyoming. 1980, pp. 341–348.
100. Bagmet, O. A., Nosochenko, A. O., Ganoshenco, I. V. Influence of Controlled Rolling on Structure and Texture Formation in Microalloyed C-Mn-Nb-V Steel. – *Acta Metallurgica Slovaca*. 2007, (13), pp.342–351.
101. EN 100021-1 2001 Metallic materials – Tensile testing – Part 1: Method of Test at Ambient Temperature.
102. Slickers, K.. Automatic Atomic-Emission-Spectroscopy. Brühlsche Universitätsdruckerei, Giessen, 1993.
103. Cemented Tungsten Carbides. Production, Properties, and Testing. Edited by Upafhyaya, G. S. Noyes Publications, Westwood, New Jersey, USA 1998.
104. Roebuck, B., Gee, M. G. Proceedings of European Powder Metallurgy Congress PM 2002. 2002, pp. 129.
105. ASTM G65 1994 Standard Test Methods for Measuring Abrasion Using the Dry Sand/Rubber Wheel.

List of publication of author

- I. **Peetsalu, P.**, Zimakov, S., Pirso, J., Mikli, V., Tarbe, R., Kulu, P. Technology and Characterization of Composite Thermal Spray Powders. – *J. Materials Science (Medžiagotyra)*. 2005, 11(4), pp. 385–389
- II. **Peetsalu, P.**, Zimakov, S., Pirso, J., Mikli, V., Tarbe, R., Kulu, P. Characterization of WC-Co Thermal Spray Coatings Based on the Composite Powders. – *Powder Metallurgy Progress, Journal of Science and Technology of Particle Materials*. 2006, 6(1), pp. 34–41
- III. Zimakov, S., Goljandin, D., **Peetsalu, P.**, Kulu, P. Metallic Powders Produced by the Disintegrator Technology. – *International Journal of Materials and Product Technology*. 2007, 28(3/4), pp. 226–251
- IV. **Peetsalu, P.**, Saarna, M., Valdek, M., Juurma, M. Computer Based Steel Microstructure Analysis Describing the Size and Distribution of Structure Phases. – *Acta Metallurgica Slovaca*. 2007, 13(1), pp. 91–95

Not included in the thesis

- V. **Peetsalu, P.**, Saarna, M., Mikli, V. Assessment of Non-metallic Inclusions in Sheet Metals by Computer Analysis. – *Proceedings of the Seventh International Conference on Clean Steel*. 4–6 June Balatonfüred, Hungary, 2007, pp. 332–341
- VI. Mikli, V., Kulu, P., Tarbe, R., **Peetsalu, P.**, Zimakov, S. Recycled Hardmetal Based Powders for Thermal Spray. – *Proceedings of the Estonian Academy of Sciences Engineering*. 2004, 10(4), pp. 315–325
- VII. **Peetsalu, P.**, Zimakov, S., Pirso, J., Mikli, V., Tarbe, R., Kulu, P. Characterization of WC-Co Composite Thermal Spray Powders and Coating. – *Proceedings of the Estonian Academy of Sciences Engineering*. 2006, 12(4), pp. 435–444
- VIII. **Peetsalu, P.**, Zimakov, S., Pirso, J., Mikli, V., Tarbe, R., Traksmaa R., Kulu, P. Characteristics of WC-Co Composite Thermal Spray Coating Microstructure. – *Congress & Exhibition Proceedings, Euro PM2006*. 23–25 Oktober, Ghent, Belgium, 2006, (1), pp. 123–128
- IX. Tarbe, R., Zimakov, S., **Peetsalu, P.**, Kulu, P., Mikli, V. Experimental Spray Powders and Coatings Produced from Recycled Hardmetal by Various Mechanical Methods. – *Congress & Exhibition Proceedings, Euro PM2006*. 23–25 Oktober, Ghent, Belgium, 2006, (1), pp. 259–264
- X. Zimakov, S., **Peetsalu, P.**, Pirso, J., Kulu, P., Mikli, V. Thermal Spray Coatings from WC-Co Powders Produced by Mechanically Activated Synthesis. – *Proceedings of International Thermal Spray Conference (ITSC) & Exposition*. 15-18 May, Seattle, USA, 2006 [CD-ROM]
- XI. **Peetsalu, P.**, Zimakov, S., Pirso, J., Mikli, V., Tarbe, R., Kulu, P. Characterization of Composite Thermal Spray Powders. – *Congress & Exhibition Proceedings, Euro PM2005*. 2–5 October Prague, Czech Republic, 2005 pp. 87–92
- XII. Kulu, P., Goljandin, D., **Peetsalu, P.**, Metal Powders Produced by Mechanical Methods. – *Proceedings of PM2004 World Congress*. 17–21 October Vienna, Austria, 2004, (1), pp. 157–162
- XIII. Mikli, V., Kulu, P., Tarbe, R., **Peetsalu, P.** Double-Cemented Recycled Hardmetal Based Powders for Thermal Spray. – *Proceedings of the 4th International Conference of DAAAM Estonia, Industrial Engineering - Innovation as Competitive Edge for SME*. 29–30th April Tallinn, Estonia, 2004, pp. 211–214
- XIV. **Peetsalu, P.**, Goljandin, D., Kulu, P., Mikli, V., Käerdi, H. Micropowders Produced by Desintegrator Milling. – *Powder Metallurgy Progress, Journal of Science and Technology of Particle Materials*. 2003, 3(2), pp. 99–110
- XV. Goljandin, D., Kulu, P., **Peetsalu, P.** Ultrafine Metal Powders Produced by Grinding from the Industrial Wastes. – *Proceedings of TMS2002 Extraction and Processing Division Meeting on Recycled and Waste*

Treatment in Mineral and Metal Processing: Technical and Economical Aspects. 16–20 June Lulea, Sweden, 2002, (1), pp. 277–284

- XVI. Kulu, P., Zimakov, S., Goljandin, D., **Peetsalu, P.** Novel Thermal Spray Powders for Corrosion and Wear Resistant Coatings. – *J. Materials Science* (Medžiagotyra). 2002, 8(4), pp. 413–416
- XVII. Kulu, P., Zimakov, S., Goljandin, D., **Peetsalu, P.** Novel Thermally Sprayed Corrosion and Wear Resistant Coatings. – *Proceedings of 3rd International Conference of DAAAM National Estonia, INDUSTRIAL ENGINEERING – new challenges to SME.* 25–27 April Tallinn, Estonia, 2002, pp. 169-172

ABSTRACT

The thesis gives an overview of methods suitable for describing WC-Co powder granules for thermal spray coatings and steel C60E for safety belt tongue production. Connections between material structure and properties are the subject analyzed in this thesis to make the decisions based on calculations.

WC-Co Composite powder particles and microstructure grains vary from a few nanometres to hundreds of micrometers. It is therefore necessary to combine different analysis methods. In the granule and particle size analysis laser diffraction, sieve analysis, image analysis and the BET method were used. To describe the microstructure and porosity of the thermal spray coating and composite powder granules, computer analysis were used.

As a result, a good numeric database was obtained that enables us to compare the characteristics of the coating with new experimental coatings and to analyze the resistance of the coating to the abrasive wear.

The mechanical- and technological properties of C60E type steels are mostly influenced by the microstructure and chemical composition. In this study different types of low alloy steels C60E are under the microstructure analysis, they are produced by different methods and hence the microstructure, mechanical and technological properties are different. To describe the steels microstructure and to determine the ferritic grain size and carbide shape and distribution classical standard based methods are used. However the minute changes in the microstructure, which can affect the materials properties, can be too small to be detected by standard method, therefore computer analysis are used.

Hardenability during the austempering process and the mechanical properties in the annealed condition are investigated. Finally, the steel composition and microstructure aspects are shown, which affect the steel mechanical- and technological properties.

Keywords: composite powder, granule size and shape, HVOF coating structure, abrasive wear resistance, computer based microstructure analysis, low alloy steel C60E, spheroidal carbides, hardenability, fineblanking, hydrogen embrittlement.

ELULOOKIRJELDUS

1. Isikuandmed

Ees- ja perekonnanimi: Priidu Peetsalu

Sünniaeg ja -koht: 31.03.1976, Tartu

Kodakondsus: eestlane

Perekonnaseis: vallaline

2. Kontaktandmed

Address: Kõla 4-2, Tallinn 10918

Telefon: 56 222 012

E-posti aadress: priidu.peetsalu@ttu.ee

3. Hariduskäik

Õppeasutus (nimetus lõpetamise ajal)	Lõpetamise aeg	Haridus (eriala/kraad)
TTÜ Mehaanikateaduskond tootmistehnika õppesuund	2003	Tehnikateaduste magister
TTÜ Mehaanikateaduskond, tootmistehnika õppesuund	2000	Tehnikateaduste bakalaureus
Ülenurme keskkool	1994	Keskharidus

4. Keelteoskus (alg-, kesk- või kõrgtase)

Keel	Tase
Eesti	emakeel
Inglise	kesktase
Vene	kesktase

5. Täiendusõpe

Õppimise aeg	Täiendusõppe läbiviija nimetus
23-24 november 2004	Eesti e-ülikool

6. Teenistuskäik

Töötamise aeg	Tööandja nimetus	Ametikoht
2003 - ...	TTÜ, Mehaanikateaduskond, MTI	Assistent
2001 - ...	TTÜ, Mehaanika ja metroloogia katselabor	Ekspert
2000 - 2003	TTÜ, Mehaanikateaduskond, MTI	Insener

7. Teadustegevus

Artiklid on toodud lk. 55-56

Teaduskonverentsil osalemised on toodud lk. 8

8. Kaitstud lõputööd
 - a) Mittemetalsete lisandite määramine metallograafilisel meetodil. Bakalaureusetöö, *Eha Kulper*
 - b) Isotermkarastatud turvavöö keele tõmbetugevust mõjutavad tegurid. Bakalaureusetöö, *Madis Juurma*
 - c) Turvavöö keelte isotermilisel karastamisel alabeiniitse struktuuri tekkimist mõjutavad tegurid. Bakalaureusetöö, *Kristel Kahr*
 - d) AS Norma pidevtermotöötlusliini töörežiimid ja neid mõjutavad parameetrid turvavöö keelte isotermkarastusel. Bakalaureusetöö, *Tiia Kallend*
 - e) WC-Co kõvasulampinnete poorsuse ja struktuuri analüüs arvutiprogrammiga „omnimet image analysis system version 5.40“. Bakalaureusetöö, *Kaarin Ratas*
 - f) Lehtmaterjali valik AS Kitmanis. Bakalaureusetöö, *Vahur Post*
 - g) Eurometallide elektroonne andmebaas. Magistritöö, *Erko Süvala*
9. Teadustöö põhisuunad
 - a) Pihustus- ja sadestuspinded (materjalid, tehnoloogia, omadused). SF0142082s02
 - b) Kulumiskindlad materjalid ja kulumine. SF0142505s03
 - c) Turvarihma detailide termotötluse tehnoloogia Lep6026
 - d) Nanopulbrid ja nanostruktuursed pinded. ETF5881
10. Teised uurimisprojektid
 - e) Mõistuse ja käega. Muinastehnoloogilised uuringud arheoloogias (raud ja tekstiilid). ETF6110
 - f) Uued kulumis-ja korrosioonikindlad termopinded. V173
 - g) WC-Co jäätmeist ülipeene- ja nanostruktuuriga kõvasulamite valmistamine. ETF6758
 - h) Ülipeened komposiitpulberpindematerjalid. G4849

CURRICULUM VITAE

1. Personal data

Name: Priidu Peetsalu

Date and place of birth: 31.03.1976 Tartu, Estonia

Citizenship: Estonian

Marital status: Single

2. Contact information

Address: Kõla 4-2, Tallinn 10918, Estonia

Phone: +372 56 222 012

E-mail: priidu.peetsalu@ttu.ee

3. Education

Educational institution	Graduation year	Education (field of study/degree)
TUT Faculty of Mechanical Engineering, Production Engineering	2003	Master of Engineering scientist
TUT Faculty of Mechanical Engineering, Production Engineering	2000	Bachelor's degree
Ülenurme Highschool	1994	Secondary education

4. Language competence/skills (fluent; average, basic skills)

Language	Level
Estonian	native language
English	average level
Russian	average level

5. Special Courses

Period	Educational or other organisation
23-24 Novembe 2004	Estonian E-University

6. Professional Employment

Period	Organisation	Position
2003 - ...	TUT, Faculty of Mechanical Engineering, Department of Materials Engineering	Assistant
2001 - ...	TUT Mechanical testing and metrology laboratory	Expert
2000 - 2003	TUT, Faculty of Mechanical Engineering, Department of Materials Engineering	Engineer

7. Scientific work

Articles are shown on the pages 55-56.
 Approbation is shown on the page 8.
8. Defended theses
 - a) Determination of content of non-metallic inclusions by metallographic method. Bachelor's degree, *Eha Kulper*
 - b) The factors that have affect on safety belt tongue tensile strength after austempering. Bachelor's degree, *Madis Juurma*
 - c) The factors affecting the formation of low bainite structure on the safety belt tongues' austempering. Bachelor's degree, *Kristel Kahr*
 - d) AS Norma's continuous conveyer type heat treatment line working mode and the factors affecting it on safety belt tongues austempering. Bachelor's degree, *Tiia Kallend*
 - e) Porosity and structure analysis of WC-Co hard coating using "Omnimet Image Analysis System Version 5.40" software. Bachelor's degree, *Kaarin Ratas*
 - f) The choice of sheet metal on AS Kitman. Bachelor's degree, *Vahur Post*
 - g) Electronic database of metals and metallic alloys. Master degree, *Erko Siivala*
9. Main areas of scientific work/Current research topics
 - a) Sprayed and deposited coatings (materials, technology, properties). SF0142082s02
 - b) Wear resistant materials and wear. SF0142505s03
 - c) Heat treatment technology of safety belt parts production I. Lep6026
 - d) Nanopowders and nanostructured coatings. ETF5881
10. Other research projects
 - e) With Mind and Hand. Studies Ancient Technology in Archaeology (iron and textiles). ETF6110
 - f) Novel Manufacturing of Wear and Corrosion Resistant Thermally Sprayed. V173
 - g) Production of ultrafine and nanostructured WC-Co hardmetals from recycled scrap. ETF6758
 - a) Ultrafine composite powders for thermal spray. G4849